Virginia Commonwealth University

VCU Scholars Compass

Development of Mechanical Cardiovascular Assist Devices for Fontan Patients: Two Novel Approaches

Sonya Bhavsar
Virginia Commonwealth University

www.manaraa.com

DEVELOPMENT OF MECHANICAL CARDIOVASCULAR ASSIST DEVICES FOR

FONTAN PATIENTS: TWO NOVEL APPROACHES

A thesis submitted in partial fulfillment of the requirements for the degree of Master of Science in Mechanical Engineering at Virginia Commonwealth University.

by

SONYA SANAT BHAVSAR
Bachelor of Science, Biomedical Engineering, Virginia Commonwealth University, 2008

Director: DR. AMY L. THROCKMORTON
QIMONDA ASSISTANT PROFESSOR, DEPARTMENT OF MECHANICAL
ENGINEERING

Virginia Commonwealth University
Richmond, Virginia
May 2010

Acknowledgement

First and foremost I express my sincerest and deepest appreciation to my committee chair, advisor, and mentor Dr. Amy Throckmorton, who embodies the motivation and spirit of true scholarly research. Her passion for scientific exploration and dedication to teaching is honorably inspirational. Dr. Throckmorton saw more in me than I ever imagined and helped me to accomplish more than I ever thought possible. Without her guidance, encouragement, and confidence in my abilities, this thesis would not have been possible.

I also offer my heartfelt gratitude to my committee members, Dr. William Moskowitz and Dr. Karla Mossi for their advice and valuable feedback. Without Dr. Moskowitz's generous donation of his time during the IRB process, interpretations of physiologic questions, and patience during my invasion of his catheterization lab, the clinical trials would have never been complete. Dr. Mossi has been so much more than a professor and mentor to me since my undergraduate education. I am extremely thankful to her in every possible way.

In addition, a thank you to all of my colleagues for their support, encouragement, and friendship throughout my time in graduate school. Thank you to Jugal, Steven,

Gopal, David, Marshall, Eddie, James, Landon and Josh for all the lunch time adventures, late night studying/grading/writing, and wonderful memories.

Finally, I thank my family for their love and support from hundreds of miles away.

Table of Contents

List of Tables

List of Figures

Abstract

DEVELOPMENT OF MECHANICAL CARDIOVASCULAR ASSIST DEVICES FOR

FONTAN PATIENTS: TWO NOVEL APPROACHES

By Sonya Sanat Bhavsar, B.S.

A Thesis submitted in partial fulfillment of the requirements for the degree of Master of
Science in Mechanical Engineering at Virginia Commonwealth University.

Virginia Commonwealth University, 2010

Major Director: Dr. Amy L. Throckmorton
Assistant Professor, Department of Mechanical Engineering

Few therapeutic alternatives exist for patients with a failing single ventricle
physiology. To address this need, this thesis project investigated two new therapeutic
alternatives, which sought to positively augment the Fontan hemodynamics. The first
modality introduced a non-invasive method of external pressure application to the lower
extremities. A clinical study (n=2) was conducted, and results indicated an increase in flow
as a consequence to an increase in transmural pressure in the lower extremities. The second
modality investigated a minimally invasive blood pump. Numerical analyses of the pump

were performed to examine hydraulic performance under physiologic conditions. The pump produced pressure rises of 1 to 25 mmHg over flows of 1 to 4 LPM, has a blood damage index less than 1% and was also found to successfully augment the hydraulic energy of the Fontan physiology. This work resulted in substantial progress to develop both modalities and address a significant human health problem. This document was created using Mircosoft Word 2007.

CHAPTER 1 MOTIVATION AND SIGNIFICANCE

1.1 Congenital Heart Defects and Diseases

Congenital heart defects are abnormalities with the heart's structure present at the time of birth caused by the incomplete or abnormal development of fetal heart during pregnancy [1, 2]. These structural defects involve the interior walls of the heart, heart valves, and arteries and veins providing blood perfusion to cardiac tissue. The irregular cardiac structure deflects normal blood flow through the heart causing flow to slow down, proceed in the incorrect direction or location, or be completely blocked. The severity of defects can range from minimal requiring little to no corrective treatment to complex with life threatening symptoms requiring medical and surgical intervention and eventually a heart transplant [3, 4].

Congenital heart defects are the most common type of birth defect. According to the 2006 March of Dimes study, each year approximately 8 million children are born worldwide with serious, life-threatening heart defects which necessitate corrective surgery [5]. The United States alone accounts for about 1 million of these children born with congenital heart defects with 40,000 requiring immediate surgical intervention [5,6]. Specific conditions include:

1. Septal Defects – holes in the wall which separates the left side of the heart from the right side of the heart allowing mixing of oxygenated and deoxygenated blood.

1

Septal defects can occur in the atria as atrial septal defects (ASD) or in the ventricle as ventricular sepatal defects (VSD). In general, a VSD is more severe and can require surgical intervention dependent on the magnitude of the defect [6-8].

2. Valve Defects – structural abnormalities of valves which control blood flow throughout the heart and to the body and lungs. Valve defects include (a) stenosis, thickening of valve flaps preventing the valve from fully opening, (b) atresia, atypical formation of the valve lacking a passage for blood flow, and (c) regurgitation, incomplete closure of the valve causing retrograde backflow of blood. Common examples of valve defects include aortic stenosis, pulmonary stenosis, pulmonary atresia, and tricuspid atresia [6, 8].

3. Coarctation of the Aorta (COA) – narrowing of a region within the aorta resulting in a significant decrease of blood flow to the lower body [6, 7].

4. Hypoplastic Left Heart Syndrome - underdeveloped structures of the left, or systemic side of the heart causing life threatening inadequate blood flow to the body. Within the first few days of the life the baby is diagnosed critically ill and requires immediate surgical intervention [2, 6, 7]

5. Patent Ductus Arteriosus (PDA) – incomplete or no closure of the ductus arteriosus (DA) blood vessel which shunts blood away from the lungs redirecting to the body. The condition causes excessive blood flow to the newborn's lungs. PDA commonly occurs in premature births [6-8]

6. Tetralogy of Fallot (TOF) – complex defect resulting from a combination of four heart defects: pulmonary stenosis, VSD, right ventricular hypertrophy, and aortic dysfunction receiving blood from both left and right ventricles [6].

7. Transposition of the Great Arteries – transposition of the pulmonary artery and aorta resulting in delivery of deoxygenated blood from the right ventricle to the body and redelivery of oxygenated blood to the lungs from the left ventricle [6, 8]

The most serious and life threatening congenital heart defects are those which involve multiple and significant malformations of the heart chambers and vasculature. Cardiovascular malformations attribute to 6-10% of all infant deaths [1, 2]. These defects represent one of the two leading causes of neonatal death and have an occurrence of approximately 1- 8 in 1000 live births with incidence of 1 in 6 infants born preterm [2]. Cardiovascular malformations have also been found to contribute to sudden infant death. Conditions such as tricuspid artresia and hypoplastic left heart syndrome prompt single ventricle anomalies, or the contingency of only one functional ventricle. The only chance of survival for these patients is a staged surgical palliation commonly known as Fontan completion [4, 9].

1.2 Fontan Physiology

Clinical interventions prior to the Fontan operative procedure involved aortopulmonary shunts and pulmonary artery bands, designed to moderate hypoxemia and congestive heart

failure. These interventions, however, cause volume and pressure overloads, often leading to chronic ventricular hypertrophy and subendocardial ischemia [10].

Repair of univentricular physiologies through the Fontan conversion is a staged surgical palliation procedure. The first stage, known as the Norwood, occurs within the first two weeks of life and provides blood flow to the lungs through a pulmonary arterial shunt [11]. Figure 1 illustrates the Norwood repair.
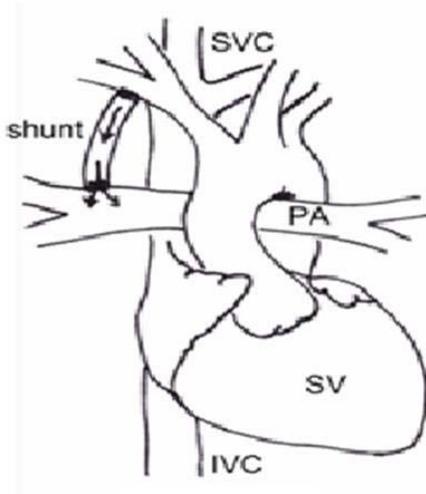
Figure 1: Norwood surgical intervention for single ventricle physiologies. A shunt is placed between aorta and pulmonary arteries to reduce blood oxygen desaturation and promote development of the pulmonary vasculature.

Once the risk of elevated pulmonary vascular resistance in the pulmonary beds has decreased the second stage, known as the Glenn, disconnects the Norwood shunt and directly connects the superior vena cava (SVC) to pulmonary circulation.

Figure 2: Glenn surgical palliative procedure providing a direct connection from the superior vena cava to pulmonary circulation. The second staged surgical palliation, referred to as the Glenn procedure, often performed after six weeks and directly connects the SVC to the pulmonary arteries.
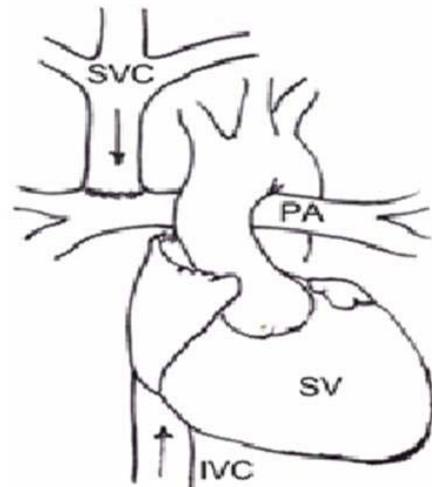
The Glenn procedure usually occurs six weeks after birth, followed by the Fontan conversion which usually occurs between the ages of 3-5 years, although each patient is unique and surgical teams complete the third stage on a case by case basis. Figure 2 shows the Glenn surgical configuration. Surgeons may decide, based on the patient's hemodynamics and body response, to remain at the Norwood, Glenn, or Hemi-Fontan stage for several years.
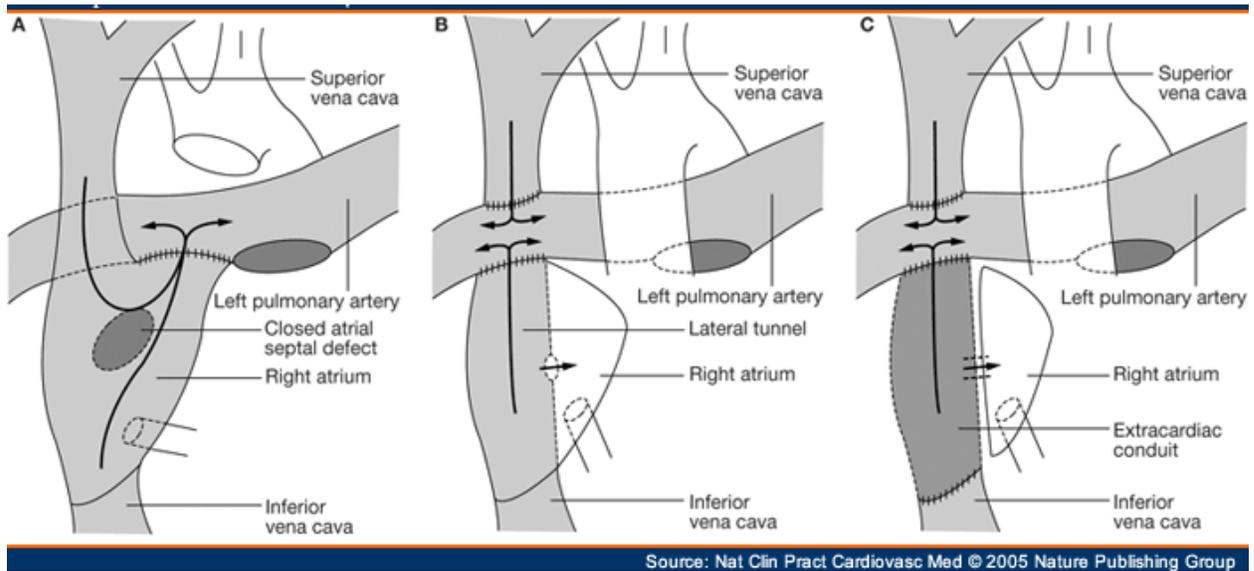
Figure 3: Variations of the Fontan surgical palliation procedure. (A) Intra-Atrial Fontan (B) Lateral Tunnel TCPC (C) Extra-Cardiac TCPC[12]

The success rate of these high risk procedures is less than 75% [11]. Each patient presents a unique challenge to surgical teams resulting in numerous modifications of these palliative procedures such as the Hemi-Fontan, Intra-Atrial Fontan, and Extracardiac Fontan as a few are demonstrated in Figure 3. The total cavopulmonary connection

(TCPC) is an example of the extracardiac Fontan first described by de Leval et al [13]. This procedure connects the inferior vena cava (IVC) and superior vena cava (SVC) directly to the unbranched right pulmonary artery [10, 14]. TCPC creates a new "man-made" physiology which entails systemic venous return transmitted directly to pulmonary circulation, formulating minimal pulsaltility of flow in pulmonary arteries [10, 15-17]. Thus, Fontan circulation is characterized by the absence of a pulmonary ventricle which is responsible for driving flow to the lungs.

Postoperative, these patients suffer from a number of associated complications due to their "man-made" physiology. Of those who survive the three staged palliation, only 85% survive the first month, 81% the first year, 79% the first five years, and 71% after 10 years [17]. Among the prevalent pathologies an increased after-load on the great veins due to elevated pulmonary pressures not only results in a significant reduction of preload reserve, but also leads to chronic conditions such as congestive heart failure and diminished exercise capacity. Decreased venous return, supraventricular arrhythmias, protein losing enteropathy, and aortopullmonary collateral vessels also plague the life-long Fontan patients [10, 15, 16, 18].

Due to the TCPC, the Fontan patient's pulmonary perfusion is reliant upon IVC pressure, thus systemic pressures are elevated to provide flow. As described by West *et al*. [19] in 1964, the upright lung is classically divided into three regions of characteristic alveolar pressure zones secondary to gravitational forces. Each zone is described by comparison to arterial and venous pressures. The superior zone demonstrates alveolar pressures greater than both arterial and venous pressures, the middle zone with alveolar

pressures less than arterial yet greater than venous pressure, and zone 3 with alveolar pressure less than both arterial and venous pressure. As can be assumed, zone 3 facilitates maximal pulmonary perfusion. Considering their decreased pulmonary vascular capacitance and correlated elevated pulmonary vascular resistance, it is likely that Fontan patients have a reduced zone 3.

A recent study performed by Lamour *et al*. [20] assessed the long term effects of age, diagnosis, and previous surgery in both adult and pediatric patients who underwent heart transplant for congenital heart disease (CHD). The multi-institutional study merged the registries from the Pediatric Heart Transplant Study (PHTS) and Cardiac Transplant Research Database (CTRD) to generate a combined dataset of patients receiving a heart transplant secondary to CHD. CTRD collected information from patients >18 years of age at the time of transplant and PHTS collected from those <18 years of age. Of the 488 CHD patients (121 from CTRD and 367 from PHTS) the last major surgical operation performed prior to transplant was the Fontan in 22% of patients and Norwood or variants of the Glenn in 21% of patients. Post transplant, patients with a previous Fontan had an 8.6-fold increase risk of death as compared to all other CHD patients. The survival rates in Fontan patients was 71% after the first year and 60% five years post transplant [20].

1.3 Pediatric Mechanical Circulatory Support

Improved management strategies could reduce the risk of developing late stage, or chronic, Fontan induced pathologies [4, 17, 18, 21, 22]. Current research indicates that by improving ventricular-vascular interactions, after-load reducing agents can improve Fontan

hemodynamics [23-26]. Several surgical interventions have been introduced to improve the quality of life, increase the time to full cardiac transplant, and raise the overall odds of survival [17, 21, 27]. Mechanical circulatory support devices have become an increasingly popular treatment option for single ventricular assistance. Historically, preference was placed on extracorporeal membrane oxygenation (ECMO) as the fundamental form of mechanical circulation in pediatrics. However, efforts have been made towards the use of ventricular assist devices (VADs) to extend the time to Fontan failure necessitating full cardiac transplantation. Statistically, VADs have been reported as improving the hospital survival rate to 89% [9, 27, 28]. Surgical re-interventions to mediate failing Fontans include interjection of baffle fenstrations, atrioventricular valve repairs, hepatic vein reinclusions, pacemaker placement, prior to full heart transplantation [21]. The incidence for ultimate full cardiac transplantation is high, though the waiting time for a donor organ can be extensive and the resulting operative mortality rate of 44% [21]. Mechanical circulatory support is critical as a bridge-to-transplant, increasing the likelihood of survival while waiting for a donor heart.

1.3.1 Extracorporeal Membrane Oxygenation (ECMO)

Extracorporeal membrane oxygenation (ECMO) is the most common resource utilized for newborn and pediatric cardiopulmonary support for patients with low refractory cardiac output, arrhythmias, cardiac arrest, persistent hypoxemia or inadequate detachment from cardiopulmonary bypass [29-33]. Primary use of ECMO is to temporarily replace lung function, heat function, or both allowing recovery of a patient's cardiopulmonary system

from an acute reversible insult or injury. Numerous studies and patient reports have been published reporting the successful use of ECMO as a bridge-to-transplant and bridge-to-surgical intervention in addition to recovery [27, 30, 34, 35]. The first successful use of ECMO for cardio pulmonary bypass was reported in 1975. Since this time, the Extracorporeal Life Support Organization, a coalition founded in 1989 to study the clinical use of ECMO, has maintained a registry of more than 30,000 patients, a majority of which were neonates presenting with respiratory failure [36, 37] . Neonates and newborns present with much higher survival rates as compared to pediatric and adult patients. This is attributed to the reversibility of the disease and absence of chronic lung and heart conditions [38, 39].

ECMO systems are complex and integrate several mechanical components [28, 39]. A sample ECMO circuit from researchers at the Congenital Heart Institute of Florida [35] is illustrated in Figure 4. System components include a roller pump, ECMO bladder, silicone membrane or hollow fiber oxygenator, heat exchanger, a centrifugal or roller pump, and IV pumps for ultrafiltrate and replacement fluid.
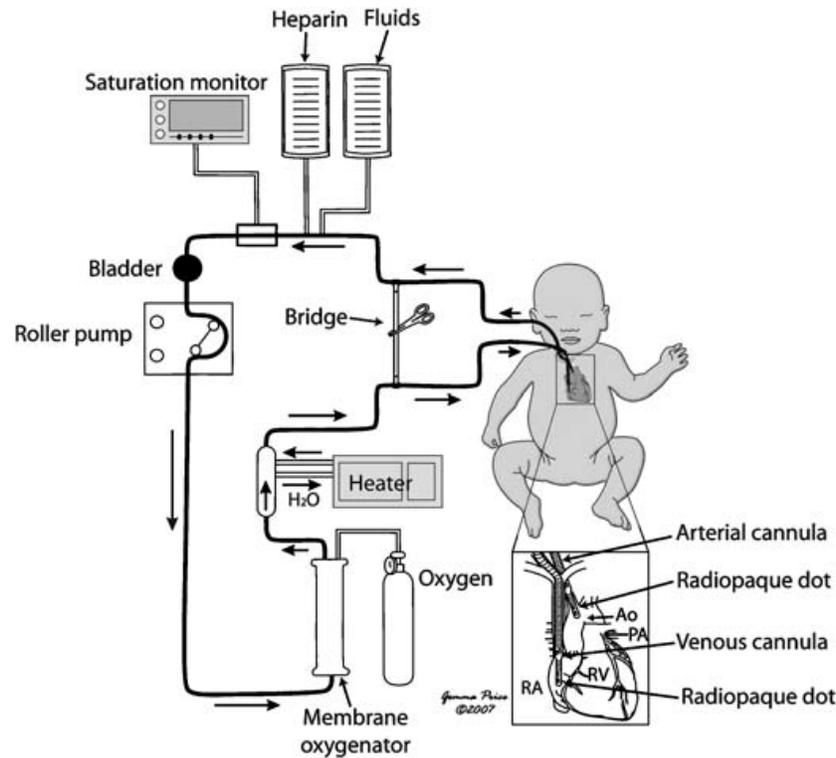
Figure 4: Schematic of a typical ECMO loop. ECMO provides hemodynamic and pulmonary support.[35]

The accumulation of numerous instruments leads the way to several possible complications and creates challenges for patients and hospital staff. An air embolism may form and could enter the arterial blood causing systemic embolization. Bubble detectors integrated into the system provide early warnings and allow hospital staff to bridge bubbles to the bladder for aspiration. Clot formations and plasma protein buildup can occur in the oxygenator membrane reducing the surface contact area for blood and gas. Additional technical failures include oxygenator failure, failure of heat exchanger, pump failure, and tube rupture [34, 35, 40].

Heparin must be continuously infused to maintain ACT between 180 to 220 seconds with calcium added to reverse CPD-A anticoagulation effects [30]. Heparin excretion is part metabolized and part intact in urine, therefore urine production has a considerable effect on apparent heparin utilization rate. The half-life of heparin in neonates on ECMO is 45 to 70 minutes. Heparin levels must be checked every morning by performing a heparin assay. Side effects from heparin include intracranial bleeding and bleeding at the cannula site [30, 41, 42].

Patients on ECMO are immobile and must remain under supervision due to the bulky complex system and propensity of complications. Average time for extubation is 24 to 48 hours and supplemental oxygen is required for the first week [40, 43, 44]. Though the oxygenator, coating material of the circuit internal surface, and blood flow controller in ECMO systems have been refined and modernized since the systems first introduction in the late 1970s, survival rates post hospital discharge in pediatric patients is approximately 50% [30, 35, 45-47] . Single ventricle physiologies have been hypothesized as one cause for high mortality rates [30, 34].

1.3.2 Ventricular Assist Devices (VADs)

While many heart pumps or ventricular assist devices (VADs) are being developed and in various stages of clinical testing, all of these blood pumps generate pressures in far excess of the desired range for cavopulmonary support. Progress in the development of pediatric VADs has achieved new milestones and continues to quickly evolve; a majority of these more compact, pediatric VADs, however, have been designed to support the

systemic circulation in a normal biventricular physiology, not to support a cavopulmonary circulation [21, 36, 48]. All of these mechanical blood pumps were designed and developed for adult or pediatric patients with congestive heart failure (CHF) and to support the systemic circulation, not the unique anatomic physiology of the cavopulmonary connection [26]. These devices produce pressures that exceed the desired range to be used for cavopulmonary support. Researchers theorize that a pressure boost of only 2 to 5 *mmHg* may be sufficient to unload the cavopulmonary circulation in adolescent and adult patients who have a failing single ventricle [49]. The rising need for alternative therapeutic options for Fontan patients created the motivation for the development of an intravascular cavopulmonary assist device.

1.3.3   Cavopulmonary Assist Devices

Several institutions have begun to pursue research and development of cavopulmonary assist devices. Rodefeld and colleagues [22] have successfully demonstrated the use of the axial flow Hemopump to assist cavopulmonary flow in animals. This research group is also developing an innovative percutaneously-implantable, expandable propeller blood pump as a cavopulmonary assist device [22]. Limitations of this design include a wide distance between the rotor and blade-tip, increasing shear stresses, and an extremely short contact time with the thin propeller blades, preventing flow control downstream. Riemer *et al*. [50] at the Stanford University have used a sheep model of the total cavopulmonary connection to test the response to the Thoratec HeartMate II axial flow blood pump (Thoratec Corporation, Pleasanton, CA). These

studies demonstrated a baseline return of cardiac output, inferior vena caval flow, and arterial pressures. Similarly, the research team at the University of Colorado has made steady progress through numerical and *in vitro* studies on the development of an axial flow pump for proposed use in the IVC only [26].

The Division of Cardiac Surgery and Department of Pediatrics at the University of Maryland Medical Center in Baltimore, MD recently published a case study on the use of the Berlin Heart for the failing Fontan, providing more evidence for the continued research and development of a VAD for single ventricle physiologies [51]. An 18-month old patient was placed on cardiac support for 179 days, at which time the VAD was removed to optimize her general status. The patient expired 55 days post-VAD removal; a dislodged tracheostomy tube was claimed the probable cause of death.

Another recent case study was performed by the Department of Cardiopulmonary Transplantation at the Texas Heart Institute at St. Luke's Episcopal Hospital involving a 14-year old male Fontan patient implanted with a left ventricular assist device as BBT. The HeartMate implantable pneumatic left ventricular assist system (IP LVAS) was implanted after the patient was placed on cardiopulmonary bypass during the operative procedure. The HeartMate IP LVAS proved full circulatory support for 45 days at which point a donor heart was available and implanted. The cardiac transplantation was a success, and the patient has remained health for more than 2 years post-transplant [52].

As proven by these research and clinical teams, the standard axial flow pump design has suitable characteristics for cavopulmonary assist. The aforementioned blood

pump designs, however, may be obstructive to flow in the event of rotational failure, and implantation requires invasive surgery.

1.4 Noninvasive Counterpulsation and Minimally-Invasive Intravascular Assist

In further support of this effort to develop alternative therapeutic options for Fontan patients, we are developing two modalities as a bridge-to-transplant, bridge-to-hemodynamic stability, bridge-to-surgical reconstruction or long-term support alternative for these patients. The first modality is an external counterpulsation system as a long-term clinical management strategy. This technology involves using commercially-available, medical anti-shock trousers on single ventricle patients. The inflation and deflation of these trousers applies circumferential pressure to the lower extremities which translates into an increase in venous return pressure and cardiac output. We speculate that this counterpulsation system will improve functional and exercise capacity in these patients.

The second modality is a collapsible, percutaneously-placed, axial flow blood pump to support the cavopulmonary circulation. Mechanical pressure augmentation of blood flow in the cavopulmonary circulation would decrease elevated systemic venous pressure and increase ventricular preload. This type of blood pump, which is specifically designed to support the unique anatomic and physiologic conditions of the univentricular circulation, has never been developed.

The intravascular, axial flow blood pump with a magnetically levitated rotor and a uniquely shaped protective cage. Figure 5 illustrates the conceptual design of the blood pump. The intravascular axial flow pump is designed for percutaneous positioning in the

inferior vena cava (IVC). The outer protective cage has radially arranged filaments that serve as touchdown surfaces to protect the vessel wall from the rotating components. Each filament is hydrodynamically designed to reduce drag and to maximize energy production from the rotating, engineered impeller blades. Currently the rotating pump consists of an impeller with four uniquely designed and helically wrapped blades to maximize energy transfer. Pump rotation is induced through a motor-magnetic bearing suspension, which levitate and rotate the impeller within the protective cage of filaments. An outlet nose is also located at the outflow of the pump to physically limit the axial movement of the impeller, to connect the cage filaments, and to house bearings which support the impeller during operation. The blade tip-to-tip diameter of the first generation design is 14 *mm* in the fully open configuration. In this study, for the purposes of measuring hydraulic performance, the pump prototype was mounted to a drive-shaft that was supported by mechanical bearings. The target design for the intravascular pump is to generate flow rates of 0.5 to 4 *L/min* with pressure rises of 2 to 25 *mmHg* for rotational speeds of 3000 to 6000 RPM.
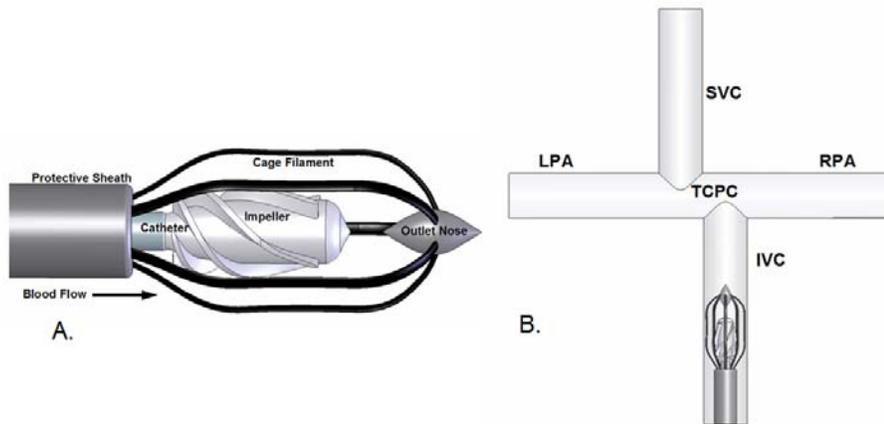
Figure 5: Conceptual Design of the Axial Flow Blood Pump. (A) The device consists of a protective sheath with cage filaments, a rotating shaft and catheter, an impeller blades, diffuser region, and inlet and outlet sections. (B) Position of the cavopulmonary assist device in the IVC of the TCPC for Fontan patients. It is designed to augment pressure and thus flow in IVC and subsequently drive blood into the left and right pulmonary arteries (LPA and RPA) while supporting the incoming flow from the superior vena cava (SVC).

1.5 Project Goal and Objectives

The goals of research for this M.S. thesis included the design, development, and evaluation of two modalities augment Fontan circulatory hemodynamics and cardiac function. A dual methodical approach to improving Fontan function was determined by the need for both preventative hemodynamic assistance and mechanical assistance to provide a bridge-to-transplant, bridge-to-surgical reconstruction, or bridge-to-recovery. The following are the objectives of this research:

1. Obtain a thorough understanding of the unique anatomy and physiology of the Fontan surgical intervention and circulatory impact

2. Determine the parameters and engineering design specifications for circulatory augmentation of Fontan hemodynamics.

3. Design and retrofit adult and pediatric size external pressure garment for a noninvasive, preventative approach for hemodynamic support for Fontan patients.

4. Contrive and compose pressure garment protocols and obtain IRB approval for MAST clinical trials.

5. Conduct MAST clinical trials on two patients during cardiac catheterizations at the Medical College of Virginia.

6. Design and conduct numerical analyses on an intravascular, axial flow blood pump for minimally invasive mechanical circulatory support for Failing Fontan physiology to serve as a bridge-to-transplant, bridge-to-surgical intervention, or bridge-to-recovery.

7. Generate computational models for the total cavopulmonary connection (TCPC) Fontan including idealized configurations and patient specific configurations derived from MRI images.

8. Conduct computational fluid dynamics (CFD) analyses on TCPC models with intravascular blood pump mechanical support.

9. Perform the following analyses: pressure-flow, blood damage, shear stress, quasi-steady state, and energy loss calculations.

This thesis project provided insights into two forms of therapeutic treatments for Fontan patients. Achievement of these objectives resulted in substantial progress in the development of both modalities to address a significant human health problem.

1.6 Thesis Outline

This thesis reports two methods of circulatory augmentation for Fontan patients. The design and development of two mechanical modalities is detailed in subsequent chapters. Chapter 2 reports the construction of a noninvasive mechanical circulatory augmentation garment designed improve hemodynamics by reducing the workload of the systemic ventricle and providing increased pressure and blood flow to the lungs. The goal of the external circulatory augmentation garment is to provide patients with a therapeutic medical device for use at home to alleviate some cardiac workload thus providing a preventative approach to combat the ensuing Failing Fontan physiology.

Chapter 3 reports the design and development of an intravascular, axial flow blood pump intended as a minimally invasive approach for mechanical circulatory augmentation of the Failing Fontan physiology. Computational fluid dynamic (CFD) analyses were performed with the pump placed in idealized and patient specific TCPC models. The results from both the counterpulsation studies and numerical simulations are reported in Chapter 4. Chapter 5 discusses the success and usefulness of both devices and indications for clinical use. Conclusions and future research expectations and goals are detailed in Chapter 6.

CHAPTER 2 METHODS AND MATERIALS: COUNTERPULSATION

2.1 Theory of External Circulatory Augmentation

Traditionally mechanical cardiovascular assist devices are invasive and designed specifically for adult patients suffering from congestive heart failure. The success of these devices in adults with CHF is well reported and discussed in earlier sections. Though these traditional mechanical circulatory support devices have been shown to mediate the failing Fontan physiology prior to full transplant, current research indicates device success as only a short term bridge to transplant, not for use over an extensive period of time [21, 23, 27, 48]. Additionally, these devices require an invasive procedure for implementation and no clinically available device to date has been designed to specifically augment the unique circulatory demands of a Fontan.

The theory of external circulatory augmentation can be contrived from studying skeletal musculature during exercise. The extension and contraction of skeletal muscle during exercise is shown to augment blood flow through a pumping action generated by the propulsion of blood forward upon muscular contraction. By applying external pressure to the extremities it is possible to mimic this pumping action.

In an attempt to achieve the goals of mechanical circulatory assistance while reducing the surgical risk and cost to patients, we venture to apply external pressure to the

19

lower limbs as a preventative measure and long-term clinical treatment for Fontan patients. In the future we plan to employ external pressure to the lower limbs from a novel medical device designed to augment venous return for patient use at home. This device will assist patients through the augmentation of systemic blood flow to the pulmonary arteries, thus reducing ventricular workload, increasing venous return and pulmonary perfusion, and reducing cardiac afterload. Our review of literature and preliminary studies provide a proof-of-concept [53-56]. Two available technologies fit the criteria for obtaining relevant data for our intended contrivance: clinical application of Medical Anti-Shock Trousers (MAS trousers) and enhanced external counterpulsation (EECP).

2.2 Historical Predecessors

2.2.1 Military/Medical Anti-Shock Trousers

The origin of MAS trousers dates back to 1903, when the developer, George Crile, discovered the concept of counterpressure for treatment of hypotension associated with surgical procedures [57]. Crile developed and constructed the first counterpressure medical device as a pneumatic double layered rubber suit designed exerted uniform pressure upon inflation. Since Crile's time, MAS trousers have been updated and are part of protocol for every ambulance to use in situations of urgent assistance to patients suffering hypovolemic shock [58]. MAS trousers apply a fixed external pressure through pneumatic means to maintain a systolic pressure of 100 mmHg through increasing impedance of blood flow to the lower extremeties.

2.2.2 Enhanced External Counterpulsation

In contrast to MAS trousers, enhanced external counterpulsation (EECP) is a non-invasive counterpulsation technique designed as a therapeutic alternative for adult patients suffering from ischemic heart diseases. Approved by the Food and Drug Administration (FDA) in 1995, EECP has been demonstrated as safe and effective in the treatment of angina. A Multicenter Study conducted by Werner et al. of more than 5000 patients from over 100 centers concluded that EECP decreases angina episodes and extends the time to an exercise-induced angina episode [56].

EECP is an electrocardiogram-triggered inflation and deflation of pressure cuffs wrapped around a patient's lower extremities. The cuffs are inflated and deflated sequentially and circumferentially, resulting in the propulsion of retrograde blood flow through the arteries thus increasing coronary perfusion during diastole (ventricular filling). Figure 6 illustrates the inflation-deflation pattern timed with the cardiac cycle.
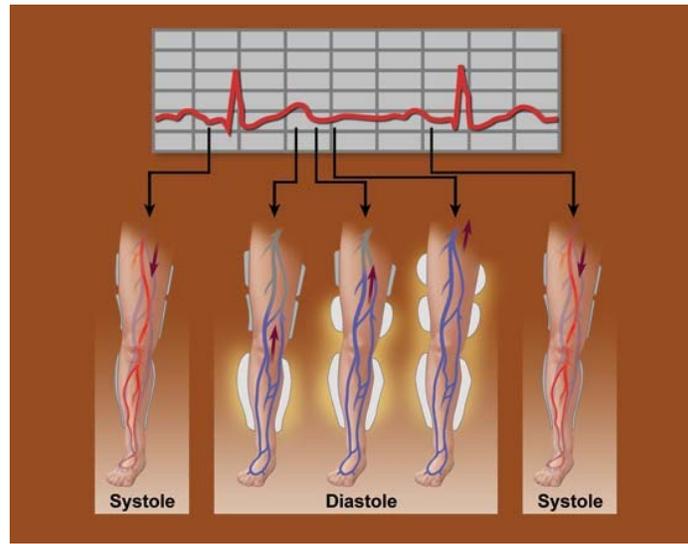
Figure 6: Electrocardiogram-trigged EECP. External pressure applied to the lower limbs is triggered by the cardiac cycle. Diastolic inflation promotes retrograde flow to the coronary arteries[59].

In 2002, Ma et al. [53] performed a clinical trial on 10 pediatric patients to assess the usefulness of using external counterpulsation early postoperatively after the Fontan conversion at the Childern's Medical Center in Dallas, TX. The study focused on the benefits of counterpulsation when applied to patients immediately postoperative for 10 minutes. Though the authors state success with safe application to pediatric patients and an increased in cardiac index, no further trials were published.

2.2.3 Application of Pulsation Technology to Fontan Patients

Due to the extensive demonstration of success in adult CHF patients, it is expected that EECP or a similar technology (i.e. retrofitted MAS trouser configuration) would have superior results on pediatric CHD patients. This assumption is based on the symptomatic and physiological similarities between these two categorical patients. Their pathological

conditions arise from the common source of poor myocardial functionality.
Counterpulsation therapy delivered with cardiac synchronization has consistently
demonstrated immediate improvement in exercise tolerance, myocardial perfusion, venous
return, and cardiac output, with several long-term benefits such as improved endothelial
function, increased peripheral oxygen uptake, and augmented ventricular systolic and
diastolic function [54, 56]. By focusing on the benefits derived from pulsation in
conjunction with simplification of the device, it is possible to develop a noninvasive,
external pulsation device for at home therapeutic use without the need for outpatient
expenditures.

Therefore, we executed a clinical study using commercially available MAS trousers on
Fontan patients. We hypothesized that routinely administered, non-invasive, external
counterpulsation will: 1) enhance flow from the great veins through the lungs, and 2) will
improve functional and exercise capacity in these patients with single ventricle physiology.
We propose to initially evaluate this hypothesis by performing a feasibility study on
pediatric patients and young adults (ages of 10 to 45) with congenital heart disease. This
study measured the increase in venous pressures and cardiac output with circumferentially
applied, external pressures on the lower extremities using commercially available medical
anti-shock trousers. Figure 7 below illustrates the location of external pressure application
via MAS trousers.
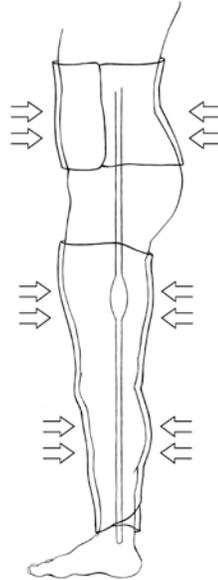
Figure 7: External pressure application to lower limbs and abdomen using MAS trousers. Hypothesized forward propulsion of blood, illustrated as a bolus in the mid-thigh above, due to external pressure to augment Fontan circulatory hemodynamic.

2.3 New Pulsation Device

Two sets of MAS trousers (David Clark Company Incorporated, Worcester, MA, U.S. Patent No. 3933150) were procured and retrofitted for the counterpulsation studies: an adult size and a pediatric size. The adult and pediatric size differed in length of lower extremity cuffs, width of the abdominal cuff, and circumferential length of the abdominal cuff. The pressure compartments on these MAS trousers were individual such that the abdominal sections were interchangeable as well as the lower extremity sections. This

provided allowance for some degree of personalized fit for the patients involved in the study. For example a tall slender subject could use the adult size lower extremity sections in conjunction with the pediatric size abdominal section.

System pressure application was provided via two means of airflow, coarse and fine adjustments, laid in series to the pressure garment. Bulk airflow to generate pressures accurate within approximately 10 mmHg originated from a standard air pump (Intertek Listed, Model: HB-505B). The air pump provided the coarse pressure adjustment to quickly elevate the pant pressure application to the patient to the desired level. A hand pump found on most sphygmomanometers was utilized for fine adjustments, elevating and relieving pressures within approximately 1 mmHg accuracy. In conjunction, the coarse and fine pressure applicators were capable of providing the external pressure application for the clinical trials.

The pressure gage was added to the system in parallel to airflow through the trousers compartments, downstream of the pump and upstream of the patient. A standard dial pressure gage found on most sphygmomanometers was used to detect and approximate trouser pressure. Figure 8 below demonstrates the design and layout of the retrofitted MAS-trousers.
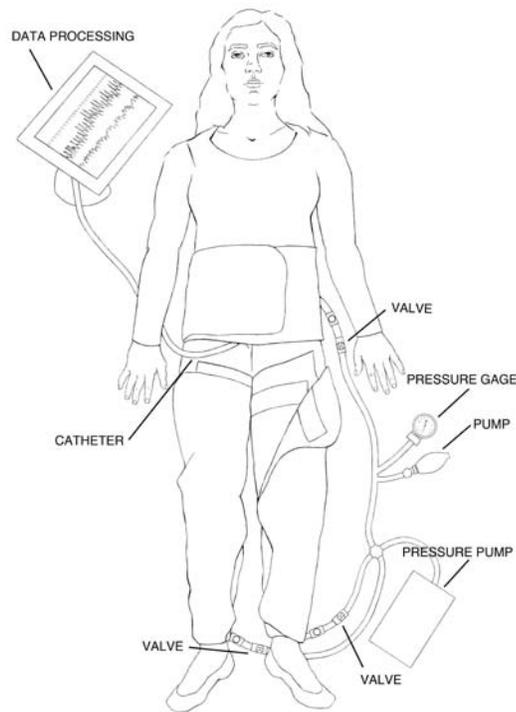
Figure 8: Schematic of retrofitted MAS trousers used for counterpulsation clinical trials.

2.4 Clinical Study

VCU Investigational Review Board (IRB) approval was obtained for this study (HM #11906). The study population consisted of volunteer subjects aged 10 to 45 years who are recruited by staff and participating personnel. All subjects had a previously scheduled, dual-sided, cardiac catheterization. To-date, two subjects have been recruited.

The subjects were examined prior to enrollment. The exclusion criteria are as follows: recent surgery or Fontan conversion within one year or less, cognitive impairment, uncontrolled arrhythmias, history of pulmonary embolism or deep vein thrombosis,

uncontrolled hypertension, uncontrolled congestive heart failure, clinically significant valvular disease (e.g. aortic regurgitation), acute myocardial infarction, excessive tachycardia or marked bradycardia, bleeding diathesis, absent pedal pulses, lower extremity and pulmonary edema, aortic aneurysm, and diaphragmatic hernia [54]. Table 1 summarizes these exclusion criteria. Neither of the participating subjects met any of these criteria.

Table 1: Exclusion Criteria for clinical trial.

Exclusion Criteria
1. *Uncontrolled Arrhythmias*
2. *Nonsustained ventricular tachycardia (NSVT)*
3. *Recent Pulmonary Edema*
4. *Recent prognosis of Deep Vein Thrombosis*
5. *Uncontrolled Hypertension*
6. *Abdominal Aortic Aneurysm > 4.0 cm*
7. *Uncontrolled Congenital Heart Failure*
8. *Acute Myocardial Infarction*
9. *Aortic Insufficiency*
10. *Mitral or Aortic Stenosis*
11. *Excessive Tachycardia*
12. *Marked Bradycardia*
13. *Bleeding Diathesis*
14. *Symptomatic peripheral vascular disease*
15. *Unsuitable deformity in lower extremity anatomy*

After obtaining informed consent, the patient was prepped for the previously scheduled cardiac catheterization. The subjects were placed in the supine position with the MAST garment applied but not inflated. A blood pressure cuff was wrapped around the patient's arm for routine measurements; a pulse oximeter was placed on the patient's index finger to measure oxygen saturation and heart rate during the study. Standard electrocardiogram leads were also appropriately located. A catheter was then inserted into the femoral vein and/or artery after the site had been cleansed and numbed with a local anesthetic, and according to the VCU standard protocol for cardiac catheterization.

Baseline measurements of blood pressure, cardiac output, respirations, right atrial pressure / central venous pressure, and pulmonary capillary wedge pressure, O_2 sat, and heart rate were taken. Based on the patient's diastolic pressure, we determined three separate pressure intervals to evaluate, up to 20 mmHg above their diastolic pressure.

After a first set of vital signs were obtained, the first pressure level was administered. The MAS trousers were inflated and a circumferential pressure was applied to the lower extremities similar to a blood pressure cuff. This pressure was held for 20 to 40 seconds and then released for 10 seconds. The pressure was applied again. These intermittently applied pressures at the first interval occurred for 3 to 5 minutes. Clinical measurements were ongoing.

At the conclusion of this 3 to 5 minute first test period, the patient's vital signs were reassessed and the MAS trousers were deflated. The patient rested for 3-5 minutes. Then, the second pressure level was tested, which is slightly higher than the first interval. The MAS trousers were inflated and a circumferential pressure was applied to the lower extremities. This second interval pressure was held for 20 to 40 seconds and then released for 10 seconds. The pressure was then applied again. These intermittently applied pressures at the second interval occurred for 3 to 5 minutes. Clinical measurements were ongoing.

At the conclusion of this 3 to 5 minute second test period, the patient's vital signs were again reassessed and the MAS trousers were deflated. The patient rested for 3-5 minutes. Finally, the third and last pressure level was evaluated. This third interval pressure was held for 20 to 40 seconds and then released for 10 seconds. The pressure was then applied

again. These intermittently applied pressures at the third interval occurred for 3 to 5 minutes. Clinical measurements of aortic systolic and diastolic pressures, pulmonary pressures, and TCPC pressure were ongoing. Upon completion, a final set of vital signs was reassessed and the MAS trousers were deflated. The patient was able to rest for 3 to 5 minutes. After 5 minutes, a final set of baseline vitals was obtained.

Deflation of the anti-shock trousers was carefully completed in order to maintain cardiac stabilization. We ensured that the subjects were not exhibiting any signs of shock and that they had a stable, strong, and regular heart rate, respirations, and blood pressure. Vital signs were carefully monitored during the deflation process.

All measurements were recorded in manner that is in compliance with IRB rules and HIPPA regulations. The subsequent table is a sample spreadsheet as indicative of the data recorded for each study.

Table 2: Sample data spreadsheet for clinical trials.

Study Number: _____   Age/Sex _____   Diagnosis _____

				Baseline Measurements			
Recording	Time	BP	HR	Resp.	O2 sat.	Left atrial / CVP	Pulmon. Cap. Wedge
1							
2							
3							
4							
5							
				Applied External Pressure of _____			
	Time	BP	HR	Resp.	O2 sat.	Left atrial / CVP	Pulmon. Cap. Wedge
1							
2							
3							
4							
5							
				Applied External Pressure of _____			
	Time	BP	HR	Resp.	O2 sat.	Left atrial / CVP	Pulmon. Cap. Wedge
1							
2							
3							
4							
5							
				Applied External Pressure of _____			
	Time	BP	HR	Resp.	O2 sat.	Left atrial / CVP	Pulmon. Cap. Wedge
1							
2							
3							
4							
5							
				Baseline Measurements			
Recording	Time	BP	HR	Resp.	O2 sat.	Left atrial / CVP	Pulmon. Cap. Wedge
1							
2							
3							
4							
5							

2.5 Chapter Summary

Counterpulsation has been shown to improve cardiovascular hemodynamics and provide symptomatic relief in adult patients suffering from CHF. Inferring from the similarities in symptoms between adult CHF patients and patients with failing Fontan physiology it was hypothesized that external pressure augmentation to the lower limbs of Fontan patients would provide them hemodynamic relief and reduce cardiac workload. An

IRB approved study was conducted over the course of Fall 2008 to Spring 2010. The clinical trial was conducted during prescheduled cardiac catheterizations and employed retro-fitted MAS trousers. Two patients were recruited and results from the clinical trials are provided in Chapter 4.

CHAPTER 3 METHODS AND MATERIALS: INTRAVASCULAR BLOOD PUMP

In contrast to the completely non-invasive and external pulsation device, another approach to augment pressure in the total cavopulmonary connection (TCPC) of Fontan patients involves the use of an intravascular blood pump. This thesis evaluated the use of such a pump in the inferior vena cava (IVC) through numerical means. The cavopulmonary assist device represents a minimally-invasive technique to support Fontan patients in the cardiac catheterization lab.

As discussed in previous chapters, repair of univentricular physiologies through the operative Fontan procedure manifests a new, "man-made" circulatory pattern for these patients deriving from a direct connection of the great veins to the pulmonary arteries. In recent years, progress in surgical advances of the TCPC has reached a plateau. Therefore, a rising interest in the implementation of an intravascular blood pump in the IVC has emerged.

Normal cardiac anatomy utilizes the right ventricle as a pumping chamber to propel blood forward into pulmonary circulation. Due to their univentricular physiology, Fontan patients have passive blood flow to the lungs. The use of an axial flow blood pump in the IVC would compensate for the loss of energy from the univentricular physiology and serve to recoup and maintain hemodynamic stability for patients suffering from a failing Fontan.

3.1 Conceptual Pump Design

In order to produce a more effective and minimally invasive bridge-to-transplant, bridge-to-recovery, or bridge-to-surgical reconstruction, we have developed a collapsible, percutaneously inserted, magnetically levitated axial flow blood pump to support the total cavopulmonary connection (TCPC) of a failing Fontan in adolescent and adult patients. Our intravascular pump would provide mechanical augmentation of blood flow from the inferior vena cava to the lungs, thus enhancing cardiovascular hemodynamics through improved systemic pressure, increased ventricular filling, and augmented cardiac output.

The axial flow blood pump is designed with a catheter-mounted impeller, diffuser blades surrounding the pump hub tip, protective cage filaments and a motor for magnetic levitation and rotation. The impeller consisted of a hub and 3 counterclockwise oriented blades and the diffuser was designed with a hub and 4 clockwise oriented blades. Figure 9 outlines the conceptual design of this pump. The development of this pump was completed through the use of pump design equations and computational fluid dynamics (CFD) analyses. One of the main objectives of this thesis was to numerically model the interactive fluid dynamics of the pump and the cavopulmonary circulation in an idealized TCPC geometry and a patient-specific TCPC geometry.
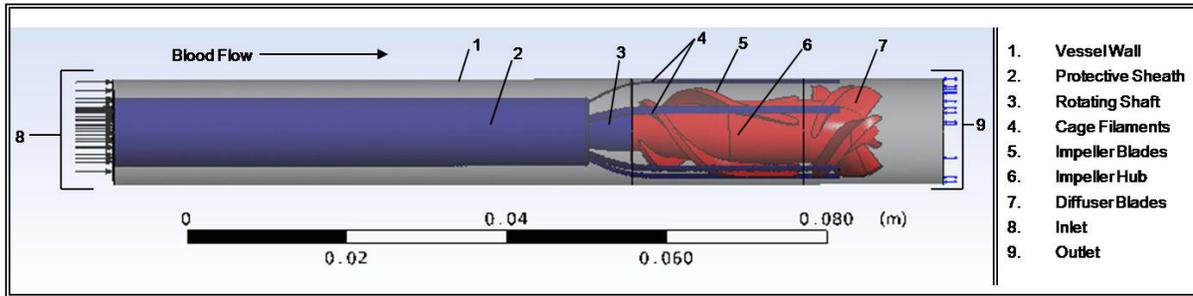
Figure 9: Intravascular Axial Flow Blood Pump for Cavopulmonary Assist. This intravascular cavopulmonary assist device consists of a protective sheath, cage filaments, a rotating shaft and catheter, impeller region and diffuser region. The axial flow blood pump was numerically modeled in a straight tube to assess hydraulic performance. Flow entered downstream of the pump at the inlet(8), traveled through the pump region, accelerated by the impeller blades(5) and exited at the outlet(9).

3.2 Methods and Materials: Computational Fluid Dynamics

3.2.1 CFD Theory

Computational fluid dynamics (CFD) has been utilized for decades to generate numerical models for blood flow though arteries, veins, stents, grafts, and blood pumps [60-63]. Numerical models serve a purpose in the design and development process by generating reliable predictors of pump performance and flow profiles. The CFD approach involves the division of a complex three-dimensional fluid domain into a congregation of smaller, discrete volumetric regions or mesh elements [64]. Mesh elements are linked at common nodes and through these connections the equations of motion can be algebraically solved. By characterization and analysis of fluid flow through each discrete node, the fluid dynamics of the entire fluid domain can be captured. Figure 10 illustrates the

computational model of the impeller region only, along with the computational element

with nodal locations.
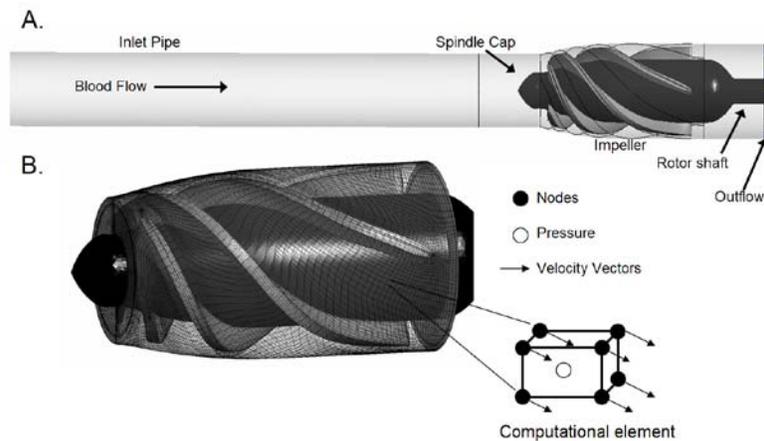
Figure 10: Computational Model of Axial Flow Impeller: A. Meshed model having four regions – inlet pipe, spindle, impeller with 4 blades, and outlet. B. Numerical analysis involves dividing the complex three-dimensional fluid model into smaller volumetric regions or mesh elements with nodes to mathematically characterize the fluid dynamics of the pump.

3.2.2 Software Programs

Several software programs were employed for the CFD work conducted during the

course of this thesis: *MIMICS* (Materialise, Leuven, Belgium), *SolidWorks* (SolidWorks

Corporation, Concord, MA), *ANSYS* (ANSYS Incorporated, Canonsburg, PA), *Bladegen*

(ANSYS Incorporated, Cansonsburg, PA) and *MatLab* (The MathWorks Incorporated,

Natick, MA). In order to assess the interactive dynamics between the pump and the TCPC

physiology, two numerical models were created: 1) an idealized TCPC geometry based on

a Ryu et al. [65], and 2) three-dimensional patient-specific models that were constructed

from magnetic resonance imaging (MRI) data of single ventricle patients. *MIMICS*

software was employed to transform two-dimensional MRI images into a three-

dimensional point cloud mesh. After numerous smoothing iterations, the three-dimensional point cloud mesh was imported into *SolidWorks* to generate a solid body model. *SolidWorks* was also utilized for the design and construction of an idealized TCPC model described by Ryu et al. [65] and elements of the intravascular pump including pump hub and protective cage. The pump impeller and diffuser blade geometries were generated using *Bladegen*. *ANSYS-CFX*, a 2nd order accurate fluid solver, was employed to simulate flow through all of the computational models. This CFD program solves the equations for the conservation of mass and momentum in terms of the dependent variables, velocity and pressure, according to the Reynolds-Averaged Navier Stokes (RANS) method. The software Matlab was used to conduct a blood damage study for various pump operating conditions.

3.2.3 Simulation Models

In order to assess the interactive dynamics between the axial flow blood pump and physiology numerical simulations were completed in two Fontan models: an idealized TCPC model generated in *SolidWorks* and a patient specific TCPC model generated in *MIMICS* and *SolidWorks*.

3.2.3.1 Idealized TCPC

A numerical model of the idealized cavopulmonary connection was constructed with the intravascular pump integrated in the inferior vena cava (IVC). This work builds upon the idealized TCPC geometry as described by Ryu et al. [65] and previous studies

with the intravascular blood pump. The following three models were analyzed: 1) an idealized TCPC with a 1-diameter offset without a blood pump, 2) an idealized TCPC with a 1-diameter offset and an axial flow blood pump having only a 3-bladed impeller, and 3) an idealized TCPC with 1-diameter offset with an axial flow blood pump having a 3-bladed impeller and 4-bladed diffuser. Pump placement for models 2 and 3 were in the IVC. Figure 11 illustrates the three idealized TCPC models.
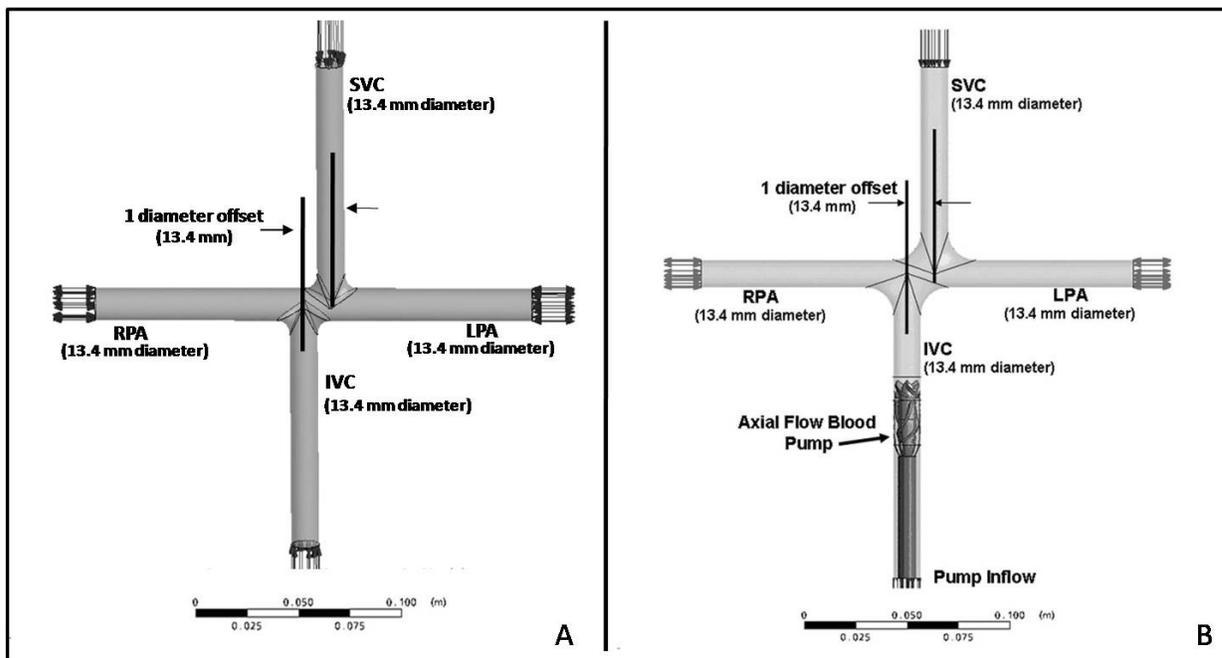
Figure 11: Idealized TCPC Models. Three idealized TCPC models were generated from geometry described by Ryu et al. IVC, SVC, LPA, and RPA vessel diameters were set to 13.4 mm. A) Idealized TCPC with no pump. B) Position of the intravascular blood pump with impeller and diffuser placed in the IVC. Since the position of the intravascular blood pump with only the impeller is so similar to B), it has not been included. The intravascular blood pump is placed in the IVC for adult patients with failing single ventricle physiology.

3.2.3.2 Anatomical TCPC

Provided that actual Fontan patient anatomy retains vascular contours and angles incapable of being captured in an idealized model, patient specific computational models were constructed from MRI's obtained from four Fontan patients. Patient number and cardiovascular anatomy are provided in Table 3.

Patient Number	Anatomy
1	Extra-Cardiac Fontan
2	Extra-Cardiac Fontan
3	Extra-Cardiac Fontan
4	Glenn

Table 3: MRI Fontan Patient Information. Four three-dimensional patient specific Fontan models were generated from patient MRI images.

Eight three-dimensional models were constructed. Models 1 through 3 demonstrated the extra-cardiac TCPC Fontan anatomy from patients 1-3 respectively. Models 4 through 6 demonstrated TCPC anatomies from patients 1-3 with an axial flow pump having a set of impeller and diffuser blades. Model 7 demonstrated a Glenn anatomy from patient 4, and Model 8 demonstrated a Glenn anatomy from patient 4 with an axial flow pump having a set of impeller and diffuser blades. Pump placement for models 1-3 were in the IVC and for model 4 was in the SVC. Figure 12 illustrates the four patient specific TCPC models. Generation of the patient specific three-dimensional solid bodies is elucidated in Figure 13 for patient 1 corresponding to model 1 and model 5.
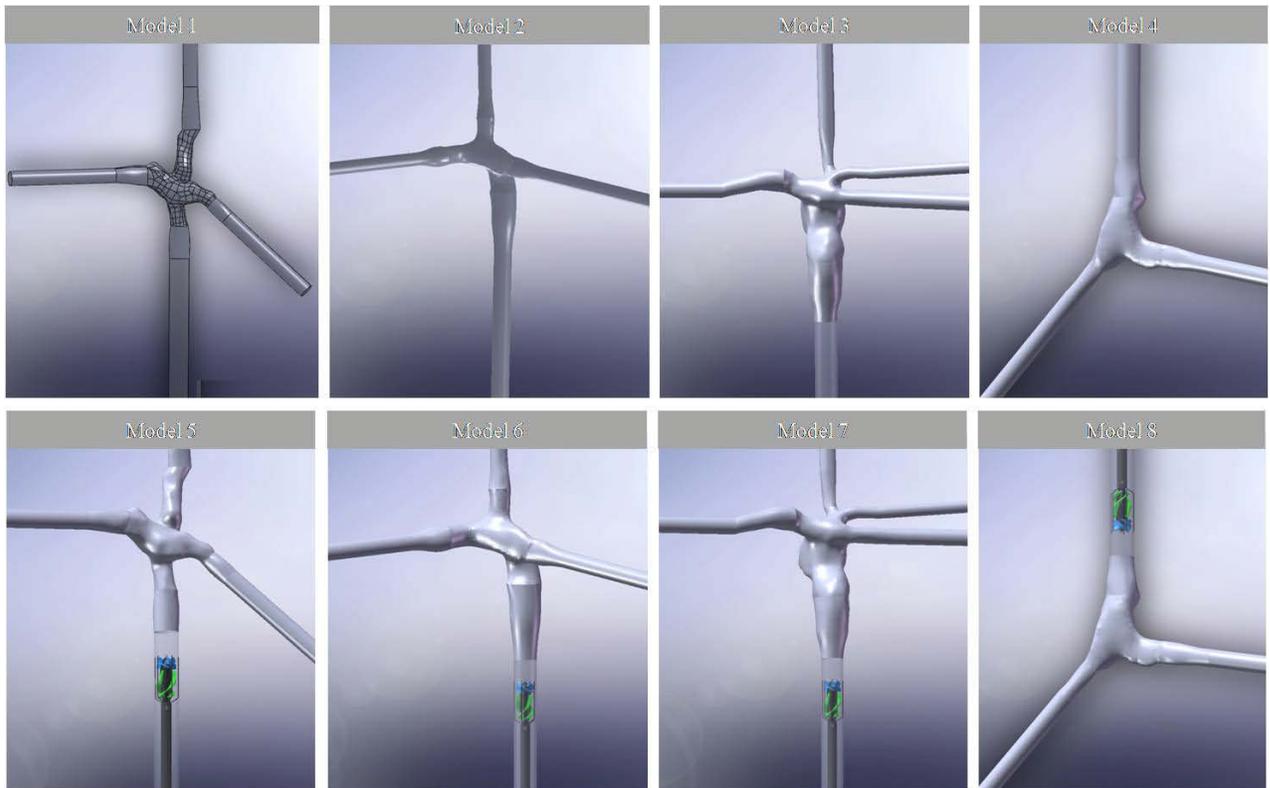
Figure 12: Patient specific anatomical TCPC models. Models 1-4 correspond to patients 1-4 respectively. Models 5-8 correspond to models 1-4 with the axial flow blood pump place in the IVC for models 5-7 and SVC in model 8.
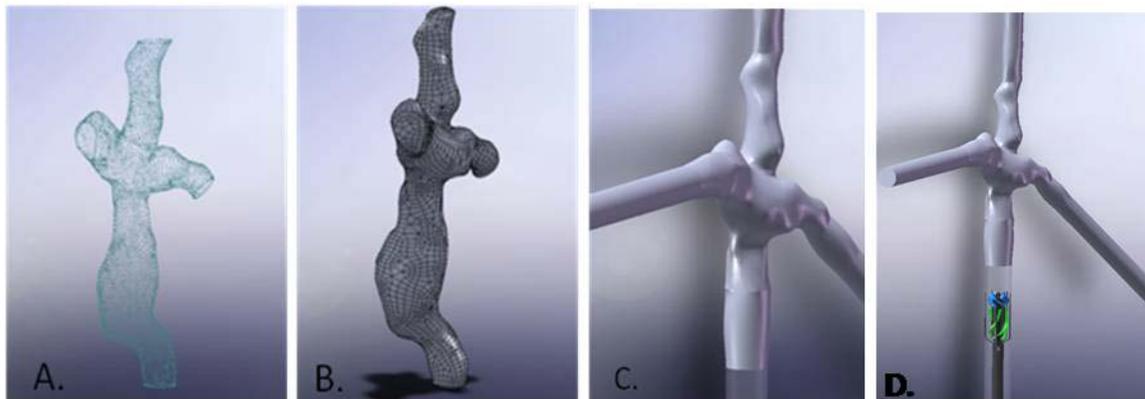
Figure 13: Generation of a patient specific computational model. A) Point cloud B) 3-D suface mesh C) Solid body anatomical model with vascular extensions D) Patient specific model with pump placement in the IVC.

3.2.4 Simulation Setup

For this thesis project, the interactive fluid dynamics of the pump and the cavopulmonary circulation were analyzed numerically an idealized TCPC geometry and one patient-specific TCPC geometry with the axial blood pump integrated into the IVC.

3.2.4.1 Grid Generation

We employed CFD software from *ANSYS* Inc. to simulate flow through all computational models. *CFX-Mesh*, an *ANSYS* mesh generation, software was used to build tetrahedral element-based meshes for the CFD analyses. Grid generation was performed by other personnel in the research laboratory. Previous grid convergence studies provided insight as to appropriate regional grid densities for the computational models [25]. Grid density and convergence studies were completed for grid quality assurance. This process included incremental adjustments to grid size until the performance results deviated less than 2%. For each simulation, the incremental time step, or relaxation factor in a steady state study, was specified as 0.001 to 0.005 with a maximum criterion of normalized convergence residual at 1×10^{-3} [61, 66].

3.2.4.2 Configuration and Boundary Conditions

Blood flow through the pump, cage, and total cavopulmonary connections was defined to be steady with constant boundary conditions and velocities for these simulations. The no-slip boundary condition was assigned to the stationary walls such that the fluid velocity values along the boundary would equal zero. A stationary wall boundary

was applied to the internal housing regions of the pump. The impeller blades and hub were specified as rotating walls in the counterclockwise direction in accordance with the blade orientation. The protective cage filaments were modeled as stationary walls, and the diffuser blades and hub were modeled to be spinning at the same speed as the impeller. The frozen rotor interface linked regions of differing reference frames between the impeller domain and protective cage [67]. A uniform mass inflow rate and rotational speed were specified for each simulation. The outlet boundary surface was specified as an opening to capture any possible irregular flow conditions at the outflow. The outlet boundary conditions, such the left and right pulmonary arteries, were defined to have static pressures of 10, 14, 18, 22 and 26 *mmHg*. All of the vessel walls for the IVC, SVC, and pulmonary arteries are modeled as rigid tubes for this initial interactive assessment.

3.2.4.3 Turbulence Model

After successful mesh generation and boundary condition specification, the computational flow model was then implemented in the 2nd order accurate fluid solver, ANSYS-CFX. This program solves the equations for the conservation of mass and momentum in terms of the dependent variables, velocity and pressure, according to the Reynolds-Averaged Navier Stokes (RANS) method. The RANS method is used to simulate the entire flow field with acceptable averaged quantities for the mean flow and fluctuating flow values. Details of the conservation of mass, Navier-Stokes equation of motion, and Reynold-Averaging procedure are outlined below.

Law of Conservation of Mass

The differential form of the continuity equation or conservation of mass is derived by the Eulerian method of analyzing the mass flow into and out of a control volume of infinitesimal size. As defined using Einstein summation convention the law of conservation of mass is [68, 69]:

$$\frac{\partial \rho}{\partial t} + \frac{\partial}{\partial x_i}\left(\rho \, U_i\right) = 0 \qquad [1]$$

where t represents time, ρ is the fluid density, and U_i is the three-dimensional velocity vector components of flow summed over the index i.

Navier-Stokes Equation of Motions

By applying Newton's law of motion to an infinitesimal fluid element, the differential form of the law of conservation of momentum is defined in Einstein summation convention as follows:

$$\frac{\partial}{\partial t}\left(\rho \, U_i\right) + \frac{\partial}{\partial x_j}\left(\rho \, U_i U_j\right) = -\frac{\partial P}{\partial x_i} - \frac{\partial \tau_{ij}}{\partial x_j} + \rho \, f_i \qquad [2]$$

where P signifies pressure, τ_{ij} is the stress tensor, x_i represent spatial variables, and f_i is the body force vector.

Neglecting the body force due to gravity, the stress tensor for a Newtonian fluid is:

$$\tau_{ij} = -\mu_b \delta_{ij} \frac{\partial U_k}{\partial x_k} - \mu_v\left(\frac{\partial U_i}{\partial x_j} + \frac{\partial U_j}{\partial x_i}\right) \qquad [3]$$

where μ_v is the dynamic viscosity, $\mu_b =$ is the bulk viscosity ($=2\mu_v$ /3), and δ_{ij} is the Kronecker delta, a symmetric identity matrix (when i=j, then $\delta_{ij} =1$, and $\delta_{ij} =0$ for i$\neq$j).

Reynolds-Averaging Procedure

The value of scalar variables fluctuate in turbulent flow conditions therefore the instantaneous value of a scalar quantity is calculated as the sum of mean and fluctuating components. Using Reynolds-Averaging, *ANSYS-CFX* expresses the instantaneous scalar quantities in terms of mean values, neglecting the fluctuating component [68]. For any arbitrary quantity θ the instantaneous scalar value is:

$$\theta = \overline{\theta} + \phi^{'} \qquad [4]$$

where θ is instantaneous scalar value, $\overline{\theta}$ is the scalar's mean component, and ϕ' represents the scalar's fluctuating component.

$\overline{\theta}$, the time-average of scalar's mean component and ϕ', the time-average of fluctuating components are defined as below:

$$\overline{\theta} = \lim_{\Delta t \to \infty} \frac{1}{\Delta t} \int_{t}^{t+\Delta t} \theta \; dt \qquad [5]$$

$$\overline{\phi^{'}} = \lim_{\Delta t \to \infty} \frac{1}{\Delta t} \int_{t}^{t+\Delta t} [\theta - \overline{\theta}] \; dt = 0 \qquad [6]$$

As observed in equation 6 the mean of individual fluctuating components is zero, but the product of fluctuating components is non-zero. For incompressible flows, the conservation of mean momentum is derived as below in Reynolds-Averaging form:

$$\frac{\partial}{\partial t}\left(\rho \; \overline{U_i}\right) + \frac{\partial}{\partial x_j}\left(\rho \; \overline{U_i} \; \overline{U_j}\right) = -\frac{\partial \overline{P}}{\partial x_i} - \frac{\partial}{\partial x_j}\left(\overline{\tau_{ij}} + \rho \; \overline{u_i^{'} u_j^{'}}\right) \qquad [7]$$

Averaging the left side of the equations using the nonlinear convection term results in the Reynolds stress tensor $\overline{\rho u_i' u_j'}$. Eddy viscosity approximations are used to relate Reynolds stress and turbulent fluctuating terms to mean flow variables resulting in the following equation:

$$\rho \; \overline{u_i' u_j'} = -\mu_t \left(\frac{\partial \overline{U_i}}{\partial x_j} + \frac{\partial \overline{U_j}}{\partial x_i} \right) + \frac{2}{3} \rho \; \delta_{ij} k \qquad [8]$$

where μ_t is the turbulent viscosity and k is the turbulent kinetic energy term.

The Reynolds-Averaged viscous stress tensor below is defined for incompressible, Newtonian fluids:

$$\overline{\tau_{ij}} = -\mu_v \left(\frac{\partial \overline{U_i}}{\partial x_j} + \frac{\partial \overline{U_j}}{\partial x_i} \right) \qquad [9]$$

The major drawback to Reynolds-averaging is the occurrence of higher order correlations between the mean and turbulent flow equations thus requiring a 'closure scheme' for these correlations or unknown turbulent stresses. Reynolds stress scheme, turbulent diffusion model, and two equation models are examples of the numerous closure models utilized for the RANS approach to model turbulent flow. Turbulence models in CFD codes solve the nonlinear Reynolds stress tensor in the Navier-Stokes equation by approximating turbulent flow conditions for the viscous dissipation and kinetic energy transfer. Turbulent viscosity,

μ_t, and turbulence kinetic energy, k, are be estimated by electing a turbulence model suitable for the defined conditions of the numerical simulations.

ANSYS-CFX has a number of different turbulence models, such as the k-ε turbulence model. The k-ε turbulence model solves the equations for k, the turbulent kinetic energy, and ε, the dissipation rate of k. The dissipation rate of k or ε is also defined as the amount of k per mass and time converted to internal fluid energy by viscous motion. Several research groups have used the k-ε turbulence model for CFD simulations to design their artificial heart pumps [60, 62, 63]. Along with the k-ε model, we selected a scalable wall function to characterize and resolve wall flow conditions.

3.2.4.4 Blood Properties

Constant viscosity values were defined for each simulation. The pump model and patient specific models were held at a constant viscosity value of 0.0035 kg/m*s corresponding to a hematocrit of approximately 33%, which reasonably represents pediatric patients suffering from congenital heart disease [70]. Hematocrit influence studies were conducted on the idealized TCPC model for three blood viscosities: 0.0035 kg/m*s, 0.005 kg/m*s and 0.0065 kg/m*s corresponding to a hematocrit of 33%, 45% and 55% respectively [62, 71]. A constant fluid density of 1050 kg/m^3 was also applied to all simulations.

The behavior of the blood in these simulations was assumed to be Newtonian [69]. At a constant viscosity Newtonian fluids demonstrate a linear relationship between shear stress and shear strain rate while non-Newtonian fluids exhibit a nonlinear relationship

between shear stress and shear strain rate. Though the heterogeneous composition of blood insinuates non-Newtonian behavior, Merrill *et al*. [72] experimentally found blood plasma to behave with Newtonian characteristics at a viscosity of approximately 1.2cP. Cokelet *et al.* [73, 74] experimentally determined that low hematocrit levels, approximately less than 50%, blood plasma demonstrates a linear relationship between shear stress and shear strain rate, thus supporting Merrill *et al.* and confirming the assumption of Newtonian behavior as acceptable.

3.2.5 Blood Damage Analysis

A blood damage analysis was performed to consider the potential for hemolysis and thrombosis for this blood-contacting intravascular blood pump. This blood damage model has been widely employed as a predictive tool in the development of several rotary blood pumps [71, 75, 76]. We used a blood damage technique that considers the three-dimensional flow field and calculates a scalar stress (σ), which includes the six components of the stress tensor and represents the level of stress experienced by the blood [77]:

$$\sigma = \left(\frac{1}{6} \sum \left(\sigma_{ii} - \sigma_{jj} \right)^2 + \sum \sigma_{ij}^2 \right)^{1/2} \qquad [10]$$

We utilized a maximum stress value of 425 *Pa* for 600 milliseconds as the design criterion in the development of axial flow VADs [25, 61, 62, 75]. We also examined fluid streamlines as indicative of numerically predicted fluid residence times within this

intravascular blood pump. Using a power law relationship between the scalar stress level and the exposure time, a blood damage index was estimated for the selected models [76], according to:

$$dHb/Hb = C \cdot \sigma^{\alpha} \cdot T^{\beta} \qquad [11]$$

where Hb is the hemoglobin content, dHb signifies the change in hemoglobin content due to blood trauma, σ corresponds to the scalar stress, T is the exposure time to the scalar stress levels, and C, α, and β reflect proportionality constants that are obtained by regressing experimental data. The accumulation of stress and exposure time was summed along the streamlines. This approach provides a statistical estimate of damage to blood cells traveling through this blood pump, according to the following power law equation:

$$D = \sum_{inlet}^{outlet} 1.8x10^{-6} \cdot \sigma^{1.991} \cdot \Delta t^{0.765} \qquad [12]$$

where *D* represents the blood damage index and indicates a 'probability' of damage to red blood cells; *t* corresponds to the stress exposure time; and *inlet* and *outlet* symbolize the entrance and exit faces in the CFD model, respectively. This model only examined the relationship between scalar stress and exposure time to the level of stress for each particle; the analysis incorporated adiabatic and isothermal conditions. To incorporate the stress history of the particles (cells), a Lagrangian tracking method was used. The particle displacement was calculated using forward integration of the particle velocity over the time step (δt):

$$x_i^n = x_i^o + \frac{dx_i^o}{dt}\delta t \qquad [13]$$

where *x* signifies the displacement and the superscripts *o* and *n* correspond to old and new

values, respectively, as the analysis moves forward along the streamlines. The numerical

constants in Equation 3, relating the stress to the exposure time, were obtained by

regression of experimental data in a Couette viscometer with an exposure time of 0.0034 to

0.6 seconds for fluid stresses of 40 to 700 *Pa* [76, 78]. This range of investigation is

comparable to the flow conditions and stress levels found in blood pumps [76, 78]. We

seek a blood damage index below 2% for our target design [79]. Table 4 lists the details of

this damage analysis, including the case number, number of particles released at the inlet

port and operating conditions.

Table 4: Blood Damage Operational Conditions. Blood damage analyses were
performed on the idealized TCPC model.

Blood Damage Cases	Flow Rate (LPM)	Rotational Speed (RPM)	Fluid Viscosity (cP)	Number of Particles
Case 1	3.5	5000	5	350
Case 2	3.5	5000	3.5	350
Case 3	3.5	4000	3.5	350

Normalized Index of Hemolysis:

Koller and Hawrylenko [80] developed an equation that is routinely used to express

blood damage in the experimental setting as a normalized index of hemolysis (N.I.H):

$$N.I.H \ (g/100L) \ = \frac{\Delta fHb \times V \times \left(1 - \left(\frac{Ht}{100}\right)\right) \times 100}{\Delta t \times Q} \qquad [14]$$

where ΔfHb is the measured increase in plasma free Hb concentration (g/L) during the test

period, Δt represents the duration of the test period (min), Ht denotes the hematocrit (%), V

corresponds to the blood volume in the test circuit (L), and Q signifies the flow rate

(L/min). This equation is employed in designing heart pumps as well as other blood-

contacting medical devices [81, 82]. The *in vitro* N.I.H values can be related to the blood

damage index according to the following equation [83].

$$N.I.H = (0.00015)(D) \qquad [15]$$

We utilized this empirical relationship to estimate the normalized index of hemolysis in the

computational models that were analyzed in this study and to compare these calculated

N.I.H values to clinically used pumps.

3.2.6 Energy Loss Calculations

To assess the impact of the blood pump in the IVC on the total energy of the

cavopulmonary flow conditions, we used the simplified control volume approach to

calculate the energy losses through TCPC configuration with and without the pump [65].

As a common approach used when considering surgical optimization of the TCPC, this

analysis allowed for the estimation of the energy loss or gain in the cavopulmonary

configuration, according to the following equation:

$$E_{loss} = -\sum (P_{static} + 0.5\rho u_k u_k) u_i n_i A_i = \sum \left(P_{total\_in}\right) Q_{inlet} - \sum \left(P_{total\_out}\right) Q_{outlet} \qquad [16]$$

$$\text{where} \quad P_{total} = \overline{P}_{static} + 0.5\rho\overline{u_i u_i} \quad [17]$$

$$Q_i = u_i A_i \quad [18]$$

In the aforementioned equations, ρ corresponds to the fluid density, P_{static} is the static fluid pressure, u_i symbolizes the components of the velocity vector, n_i is the components of the outward surface normal vector of the control surfaces, E_{loss} represents the rate of energy consumption within the control volume, P_{total} is the total pressure including the static pressure component in addition to the kinetic energy component, and Q_i is the flow rate at an inlet or outlet. A model of the TCPC alone with no pump in the IVC was created to directly compare the energy calculations to the model of the TCPC with a blood pump (impeller and diffuser) in the IVC.

3.2.7 Simulation Execution

Steady state simulations were completed on the idealized TCPC model and patient specific TCPC model with and without the axial flow blood pump inserted into the IVC.

3.2.7.1 Steady State Simulations

Over 900 numerical simulations were performed as part of this thesis project. Three main categories of operating conditions were investigated for both the idealized and patient specific TCPC models: blood flow rate, pulmonary arterial pressure, and pump rotational speed.

Blood flow rate considerations are critical to the development of any cardiovascular assist device. The average resting cardiac output (CO) for pediatric and adult patients ranges from 1 to 8 liters per minute (LPM) [12, 61, 65]. Venous return (VR), or the flow of

deoxygenated blood from the body back to the heart, emerges to the cardiac musculature via two great caval veins: the superior vena cava (SVC) and the inferior vena cava (IVC). The superior vena cava returns deoxygenated blood from the head and upper body and the inferior vena cava returns deoxygenated blood from the torso and lower body. Under steady-state conditions VR equals CO where VR is the sum of SVC and IVC flows. Deriving from anatomical characteristics, VR is dominated by IVC flow for pediatric and adult patients and almost equally shared by IVC and SVC flows for newborns and infants. For infants IVC:SVC flow is approximately 50:50 and for pediatric and adults IVC:SVC flow is approximately 60:40 to 70:30 [12, 65]. The axial flow blood pump simulated for this thesis work is designed to augment venous return of pediatric and adult Fontan patients and consequently numerical simulations were conducted for flow rates of 1 to 8 LPM distributed 60% IVC flow and 40% SVC flow.

Pulmonary arterial pressure considerations were also essential to accurate numerical modeling of the Failing Fontan physiology. On account of the Fontan single ventricle driving systemic blood flow, VR is transmitted directly to pulmonary circulation. Considering the cardiovascular system as a closed system, IVC and SVC flow must overcome pulmonary vascular resistance resulting in an increased after-load on the great veins whereas in normal biventricular circulation mean caval pressures are less than 10 mmHg and mean arterial pressures are at least 15mmHg [12]. This thesis blood pump is designed to provide an after-load reducing agent to improve the Failing Fontan hemodynamics and therefore must be numerical simulated under elevated pulmonary

resistance conditions. Numerical simulations were conducted for the pressure range 10 mmHg to 26 mmHg in the left pulmonary artery (LPA) and right pulmonary artery (RPA).

The third major operational condition investigated was the axial flow blood pump rotational speeds. Pump rotation is used to impart kinetic energy on blood flow and is influential to the pump's ability to alleviate the poor hemodynamics of the Fontan physiology. Pump performance to augment venous return is a function of rotational speed and must be considered over a range of pressures and flow rates. Optimization of pump design with regard to implementation of diffuser blades and diffuser bladed orientation were also determined in part by rotational speed influence. Numerical simulations were conducted for rotational speeds of 1000 to 8000 RPM.

In order to determine the effect of blood viscosity on pump performance, steady state numerical simulations completed on the idealized TCPC model were performed with 3 blood viscosities: 3.5cP, 5.0 cP, and 6.5 cP corresponding to hematocrits of 33%, 45%, and 55% respectively [70]. Parameters included all three major operational conditions as disclosed in the preceding paragraphs.

Fluid particle streamlines and scalar stress values were examined to predict the potential of hemolysis and thrombosis due to blood contact with the pump. 350 fluid particles were released at the IVC inlet of the idealized TCPC model for each of 3 blood damage cases aforementioned in Table 5. Of the 3 damage cases reviewed, 1 was at the pump design point (Case II) and 2 were off-design point (Case I, III). Off-design point damage indices were examined since the pump will often be operating off-design. Particle

residence time on the streamline and scalar stress exposure during contact with the pump and irregular flow patterns were used for the damage index calculations.

Energy gain calculations for both the idealized TCPC model and the patient specific TCPC model were completed by conducting simulations on the TCPC models without the axial flow blood pump. Parameters for the model simulations without pump included pulmonary arterial pressures of 14 mmHg, fluid viscosity of 3.5 cP, and flow rates of 1 to 4 LPM in the SVC and IVC.

3.2.7.2 Quasi-Steady State Studies

A quasi-steady state study was performed on the idealized TCPC model with the 3-bladed impeller and 4-bladed diffuser axial flow blood pump. The purpose of this study was to determine the optimal position for the diffuser blades to maximize pressure generation and to reduce flow vorticity at the outlet. The diffuser blades were incrementally rotated by 3° and a new grid was created for the diffuser blades at each rotational position. The new grid at each rotation increment was of the same size (within 1%) and of the same grid quality as compared with the original diffuser model. The new meshes for the diffuser at each degree increment were then incorporated into the overall model and a new simulation was completed. Due to the four bladed geometry of the diffuser region, the achievement of a 90° incremental rotation captures the quasi-steady performance of the blades. Additional rotations above 90° would be unnecessary given the symmetry of the diffuser region. The boundary conditions in these simulations remained the same as for all other simulations conducted during this thesis. 30 different rotational

geometries and meshes were generated and evaluated for the diffuser region. The numerical simulations was conducted on the idealized TCPC model with a flow rate of 2 LPM, pulmonary arterial pressures of 14 mmHg, pump rotational speed of 5000 RPM, and blood viscosity of 3.5 cP correlating to a hematocrit of 33%.

3.2.7.3 Simulations Completed

Numerical simulations completed for pump performance in the idealized TCPC model and patient specific TCPC model are summarized in Table 5, 6 and 7 below.

Table 5: Summary of steady state numerical simulations.

Fontan Model	Pump Rotational Speed	LPA/RPA Pressure	Flow Rate	Blood Viscosity
Idealized TCPC	1000 -8000 RPM	10 – 26 mmHg	1 – 8 LPM	3.5cP, 5cP, 6.5cP
Patient Specific TCPC	1000 – 5000 RPM	14 – 22 mmHg	1 -5 LPM	3.5cP

Table 6: Summary of quasi-steady state numerical simulations. Simulations were completed with the idealized TCPC model.

Parameter	Value
Impeller Region	3 Blades
Diffuser Region	4 Blades
Rotational Increments	3°
Flow Rate	2 LPM
LPA/RPA Pressures	14 mmHg
Pump Rotational Speed	5000 RPM
Blood Viscosity	3.5 cP

Table 7: Summary of blood damage analyses numerical simulations. Simulations were completed with the idealized TCPC model at steady state.

Blood Damage Cases	Flow Rate	Rotational Speed	Fluid Viscosity	Number of Particles
Case 1	3.5 LPM	5000 RPM	5 cP	350
Case 2	3.5 LPM	5000 RPM	3.5 cP	350
Case 3	3.5 LPM	4000 RPM	3.5 cP	350

3.3 Chapter Summary

This chapter discussed the software employed to design and conduct numerical analyses on a minimally invasive approach for providing hemodynamic relief and a bridge-to-recovery, -transplant, or -surgical reconstruction to patients with Fontan physiology. The axial flow blood pump was numerically simulated in an idealized TCPC model and patient specific TCPC model for performance evaluation under varying physiologic conditions and pump rotational speeds. Tablatures of all completed simulations were provided. The subsequent chapter provides results for both modalities investigated for this thesis work.

CHAPTER 4 RESULTS

4.1 MAST Clinical Trial Results

Results from this clinical trial with two patients (n=2) agree with literature in that MAS trousers successfully augmented venous return, systemic pressure, cardiac output, and blood pressure [55, 57, 84, 85]. Both patients demonstrated significant augmentation in pressure levels during external pressure application. Common trends with both patients included an increase in cardiac pressure during inflation holds and return to baseline during deflation holds. The cyclic inflation/deflation cycles are clearly visible for patient 1; patient 2 data reflected the cyclic inflation/deflation during the upper range of external pressure application. This discontinuity between patient cardiac reactions is discussed in full in the discussion section.

4.1.1 Pressure Augmentation

The three external pressures were applied to the lower limbs of both patients and abdominal section of patient 1 were determined based upon mean baseline calculations. Mean baseline diastolic pressure for patient 1 was 47 mmHg; external pressure application consisted of cyclic inflation/deflation at 37 mmHg, 47 mmHg, and 57 mmHg with rudimentary rest periods between each level. Patient 2 had a mean baseline diastolic pressure of 79 mmHg and the external application was cycled at 69 mmHg, 79 mmHg, and

89 mmHg with similar rests periods between each level. Table 8 below outlines patients'

baseline measurements and applied external pressure levels.

Table 8: Patient baseline and applied external application data.

Patient	Age	Gender	Cardiac Anatomy	Baseline Aortic Pressures (mmHg)			1st Pressure Cycle (mmHg)	2nd Pressure Cycle (mmHg)	3rd Pressure Cycle (mmHg)
				Systolic BP	Diastolic BP	MAP			
1	37	female	Extra-Cardiac Fontan	94	47	63	37	47	57
2	24	male	Intra-Atrial Fontan	117	79	92	69	79	89

Patient 1 developed measurable pressure augmentations during all three external

pressure levels; increase in cardiac pressure ranged from approximately 9-15 mmHg in

systolic blood pressure, 4-10 mmHg in diastolic blood pressure, and 5-11 mmHg in

calculated VMAP. Average hemodynamic improvements to patient 1as determined by

pressure increase ranged from 10% during the first cycle at 37 mmHg external pressure to

20% during the third cycle conducted at 57 mmHg external pressure. Figure 12 illustrates

average pressure augmentation measured at the aortic arch as a function of external

pressure application.
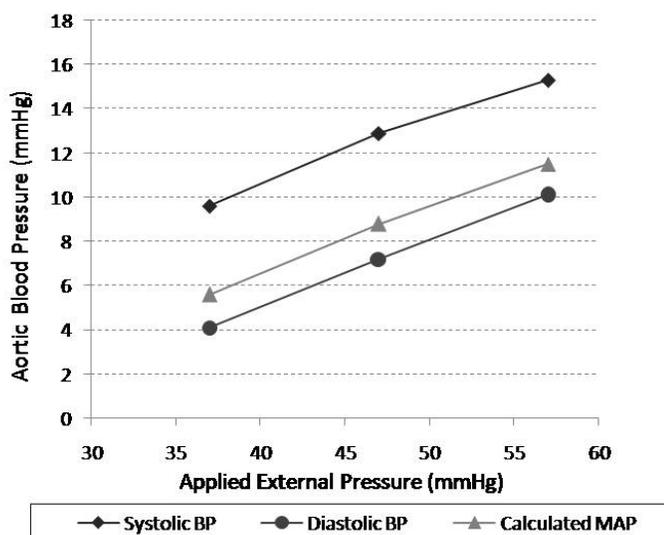
Figure 14: Patient 1 aortic augmentation to baseline pressures as a function of applied external pressure.

Patient 2 also developed detectable pressure rises during cycles of external pressure application demonstrating systolic pressure augmentation of approximately 10 -13 mmHg, diastolic increase of 5-7.5 mmHg and improvements to calculated VMAP of 3 – 9 mmHg. Patient 2 reported lower levels of hemodynamic improvement with dynamic inconsistencies and unexpected trends discussed further in Chapter 5. Figure 13 illustrates the average increase in blood pressure as a function of the external pressure application. Table 9 below outlines the average pressure augmentation for both patients as compared to the initial baseline measurements.
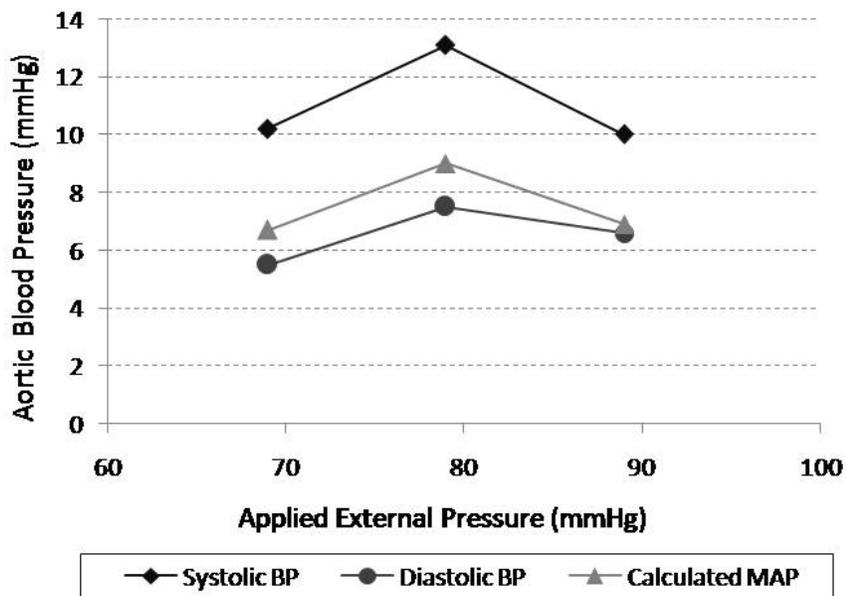
Figure 15: Patient 2 aortic augmentation to baseline pressures as a function of applied external pressure.

Table 9: Average augmentation to systolic, diastolic, and calculated VMAP blood pressures of patient 1 and patient 2 as compared to baseline measurements. Tabulated pressures reflect measured quantities obtained at aortic arch of both patients.

	Cycle Number	External Pressure Application (mmHg)	Systolic BP (mmHg)	Systolic Augmentation (mmHg)	Systolic Augmentation (%)	Diastolic BP (mmHg)	Diastolic Augmentation (mmHg)	Diastolic Augmentation (%)	MAP (mmHg)	MAP Augmentation (mmHg)	MAP Augmentation (%)
Patient 1	Baseline	0	82	--	--	47	--	--	59	--	--
	1	37	91.6	9.6	11.7	51.1	4.1	8.7	64.6	5.6	9.5
	2	47	94.9	12.9	15.7	54.2	7.2	15.3	67.8	8.8	14.9
	3	57	97.3	15.3	18.7	57.1	10.1	21.5	70.5	11.5	19.5
Patient 2	Baseline	0	117	--	--	79	--	--	92	--	--
	1	69	127.2	10.2	8.7	84.5	5.5	7.0	98.7	6.7	7.3
	2	79	130.1	13.1	11.2	86.5	7.5	9.5	101	9	9.8
	3	89	127	10	8.5	85.6	6.6	8.4	98.9	6.9	7.5

All systolic and diastolic pressures are functions of aortic pressure obtained from a catheter mounted pressure transducer placed in the aortic arch of both patients. Increases in aortic pressures were noticeable in patient pressure waveforms generated from the pressure transducer floating in the aorta. Figure 16 illustrates the increase in aortic pressures due to external pressure application for patient 1 and patient 2 during a selected inflation cycles. Figure 17 illustrates the calculated aortic MAP augmentation during 1 inflation/deflation cycle for patient 2.
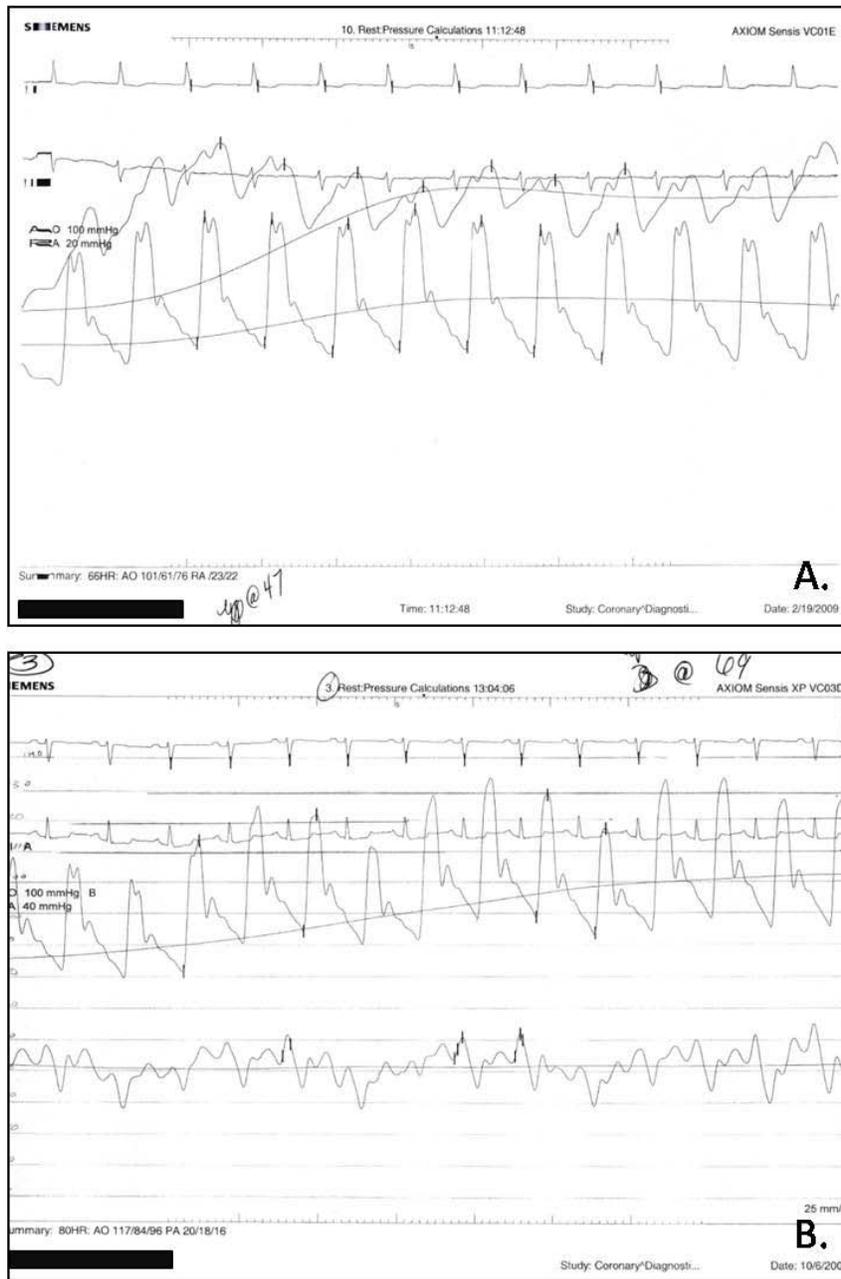
Figure 16: Sample pressure data from external pressure augmentation obtained during cardiac catheterization. A) Patient 1 during upstroke of external pressure application at 47 mmHg. B) Patient 2 during upstroke of external pressure application at 69 mmHg.
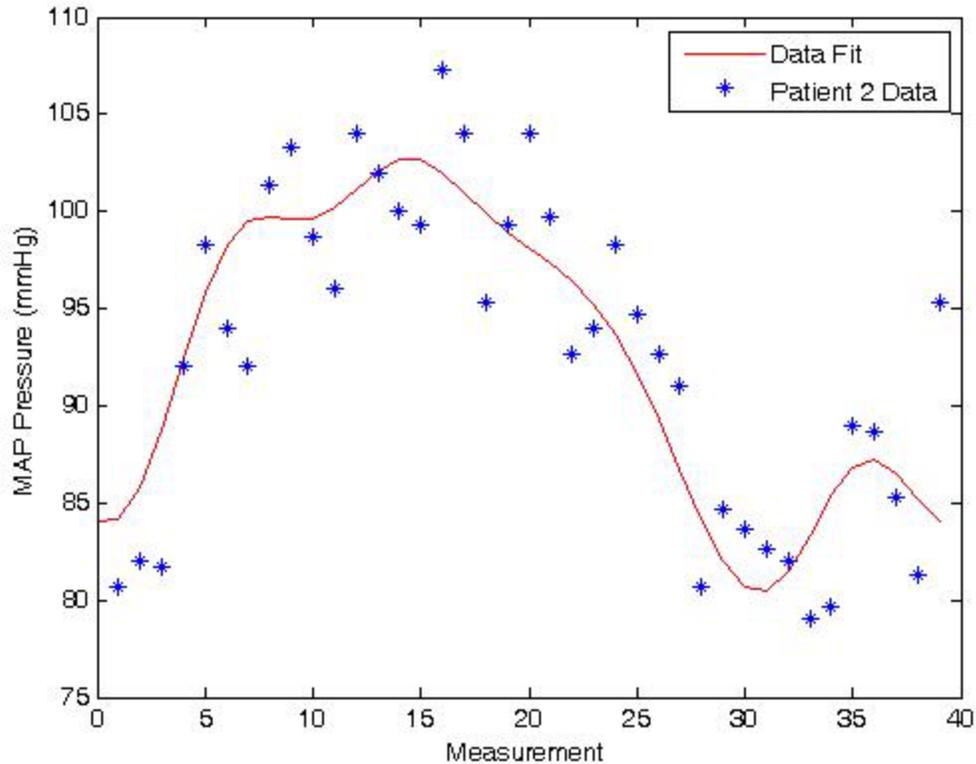
Figure 17: Aortic MAP augmentation during 1 cycle for patient 2.

4.2 Numerical Simulation Results

Figure 18 illustrates the percutaneous, magnetically levitated and rotated axial flow

blood pump designed as the minimally invasive approach for augmentation of Failing

Fontan hemodynamics. Over 900 numerical simulations were completed to optimize pump

design and test pump performance, quantifying its effectiveness at augmenting flow and

providing hemodynamic relief to Fontan patients. Simulations were conducted in 2 extra-

cardiac three dimensional models, an idealized TCPC and a patient specific TCPC

generated from MRI data, investigating multifarious physiologic conditions including

combined IVC and SVC flow rates of 1 to 7.5 LPM, pulmonary arterial pressures (LPA

and RPA) of 10 to 26 mmHg, and blood viscosities of 3.5cP, 5.0 cP, and 6.5cP. The follow

sections detail the results from these simulations.
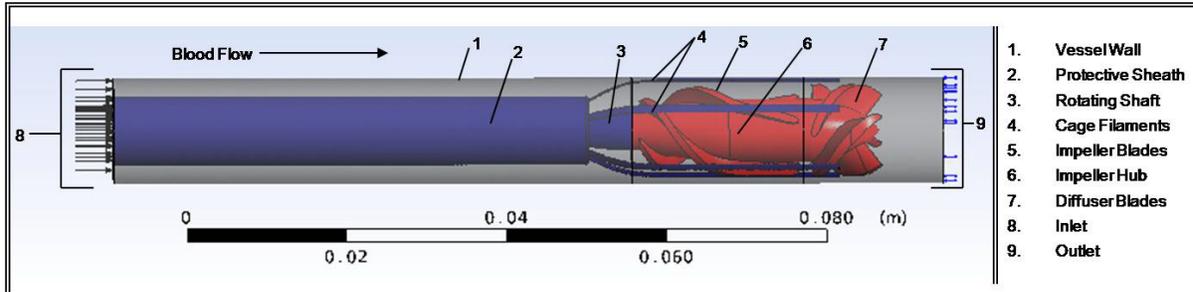
Figure 18: **Intravascular, magnetically levitated and rotated, axial flow blood pump.**
Pump is designed to provide a minimally invasive method to alleviate poor hemodynamic
associated with Failing Fontan physiology.

4.2.1 Pump Pressure Curves

The pressure generation across the intravascular blood pump in the idealized TCPC

model was determined for flow rates of 1 to 7.5 LPM and pump rotational speeds of 3000

to 8000 RPM. Figure 19 illustrates the hydraulic performance of the idealized TCPC

model. Each data point is indicative of a steady state simulation at a specific flow rate and

rotational speed. The pump delivered a range of pressure rises from 2 to 26 mmHg for

these operating conditions. Additionally, pressure rise across the pump increased with an

increase in rotational speed and decreased with an increase in flow rate, as to be expected.

The pressure curves demonstrate the axial flow pump's capabilities to provide acceptable

pressure generation for the physiologic conditions.
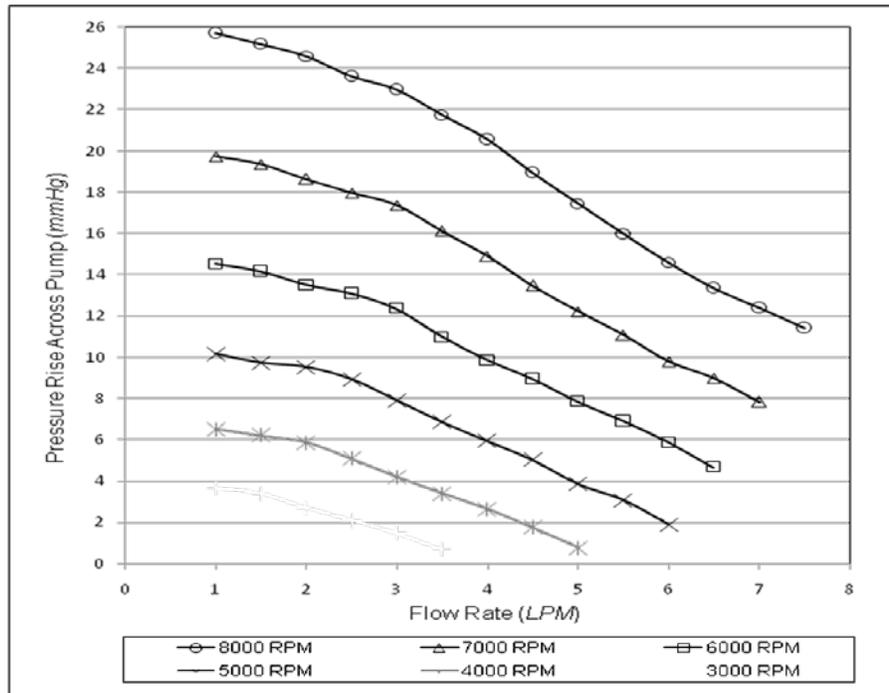
Figure 19. CFD predictions of the hydraulic performance of the blood pump in the Idealized TCPC model. Pressure generation across the axial flow blood pump with impeller and diffuser blades. Simulations were completed with flow rates of 1 to 7.5 *LPM*, rotational speeds of 3000 to 8000 *RPM*, and pulmonary arterial pressure set at 14 mmHg.

Figure 20 compares the axial flow blood pump design with and without a set of diffuser blades located at the pump head. The model with diffuser blades operated at reduced rotational speeds and generated more than twice as much pressure head across the pump. The pump with diffuser blades outperformed the pump without diffuser blades over both investigated units (flow rate and rotational speed) thus demonstrating an improvement to previous pump design work.
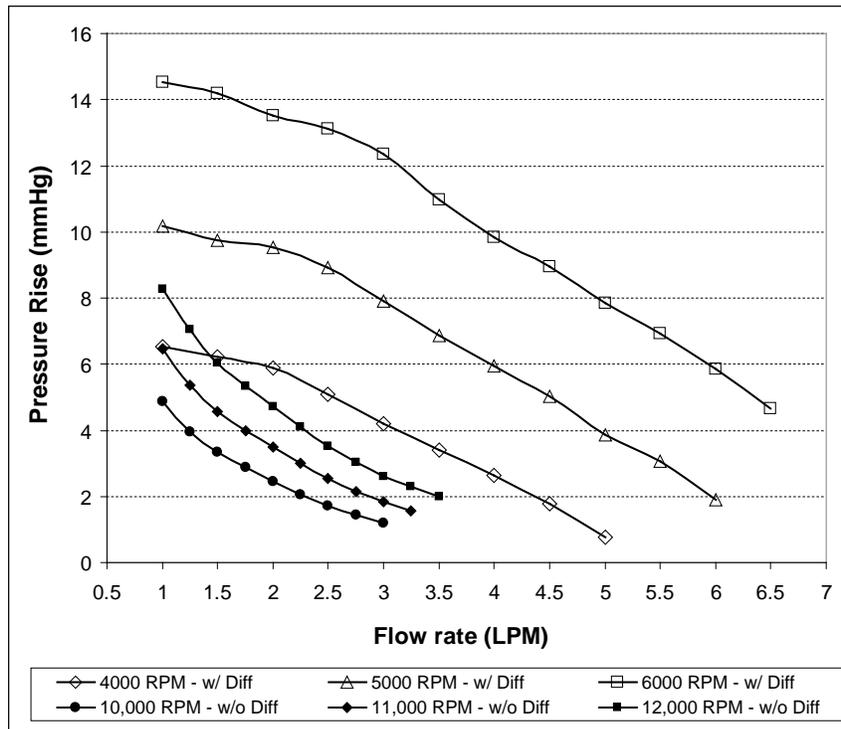
Figure 20: CFD predictions of the hydraulic performance of the blood pump in the Idealized TCPC model. Two blood pump designs were considered. One model had the protective cage, catheter, and an impeller blade set only. The other model included a set of diffuser blades at the outflow of the pump. Flow rates of 1 to 6.5 LPM were simulated for a wide range of rotational speeds of 4000 to 12,000 RPM.

The diffuser blades increased pressure rise across the pump by reducing the fluid velocity thus transferring energy to pressure as in accordance with conversation laws. Figure 21 below illustrates the reduction in fluid velocity of blood flow exiting the impeller region and associated total pressure contour across the pump. Fluid velocity augmented by rotating impeller blades was reduced by the counter orientated rotating diffuser blades, transferring the velocity augmentation to pressure augmentation.
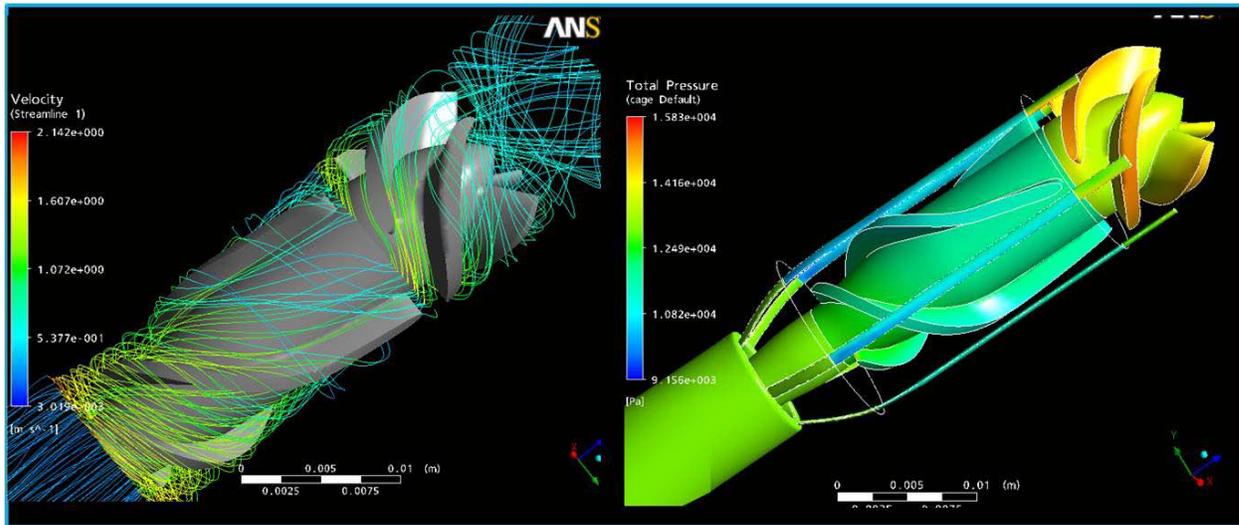
Figure 21: Diffuser blades reduce fluid velocity and increase pressure.

Figure 22 illustrates pressure rise across the pump and pressure decrease at the IVC inlet as a function of pump rotational speed for the idealized TCPC. Conditions for the comparison included flow rates of 1 to 4 *LPM* for rotational speeds of 2000 to 6000 *RPM* and pulmonary pressures of 10 to 26 *mmHg*. The IVC pressure is decreased as the pump is rotated faster, as would be expected. Additionally, higher arterial pressures lead to higher IVC pressures.
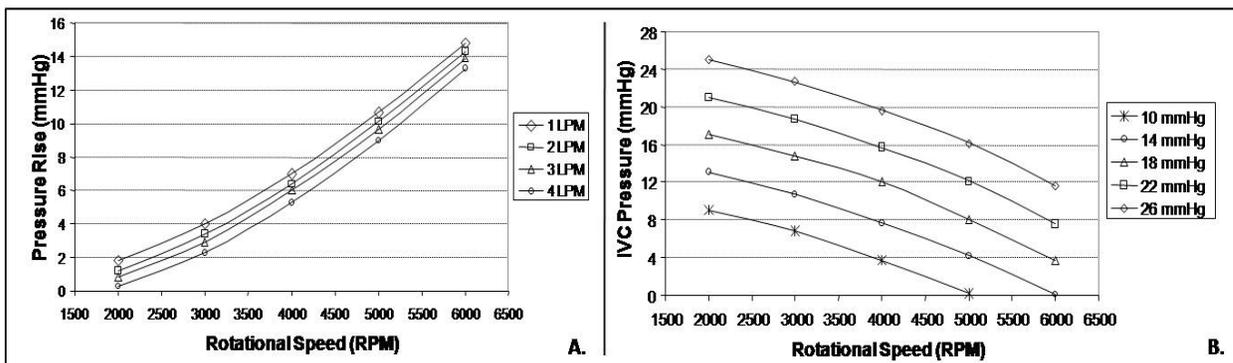
Figure 22: Pressure rise across the axial blood pump in the idealized TCPC model and the IVC pressure as a function of increasing rotational speed. (A) This graph illustrates the trends of the pressure rise across the pump to increase with increasing rotational speeds, as would be expected. In addition, the pressure rise is lower for a higher flow rate at a given rotational speed, as would theoretically be expected. (B) This graph shows the impact of the blood pump on the IVC pressure on the inlet side of the pump as a function of increasing rotational speed and pulmonary arterial pressures at a blood flow rate of 5 LPM.

The pressure generation across the intravascular blood pump in the anatomical patient specific TCPC model was determined for flow rates of 1 to 5 LPM and pump rotational speeds of 2000 to 5000 RPM. Figure 23 illustrates the hydraulic performance of the anatomical TCPC model. The pump delivered a range of pressure rises from 1 to 7 mmHg for these operating conditions. As observed in the idealized TCPC model, pressure rise across the pump increased with an increase in rotational speed and decreased with an increase in flow rate.
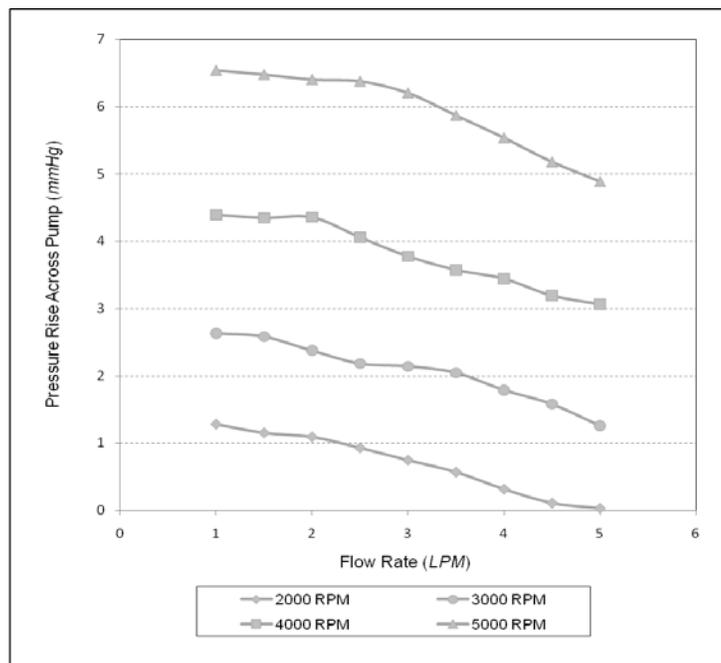
Figure 23: CFD predictions of the hydraulic performance of the blood pump in the Patient Specific TCPC model. Pressure generation across the axial flow blood pump with impeller and diffuser regions. Data represents simulations conducted at LPA=RPA=14 *mmHg* for flow rates of 1 to 5 *LPM* and pump rotational speeds of 2000 to 5000 *RPM*.

Figure 24 demonstrates the influence of pump rotational speed on IVC inlet pressure for the anatomical TCPC model. As expected, pressure at the IVC inlet decreased as a function of increased pump rotational speeds. Parameters for these results included

flow rates of 1 to 5 LPM, pump rotational speeds of 2000 to 5000 RPM and

LPA=RPA=14mmHg.
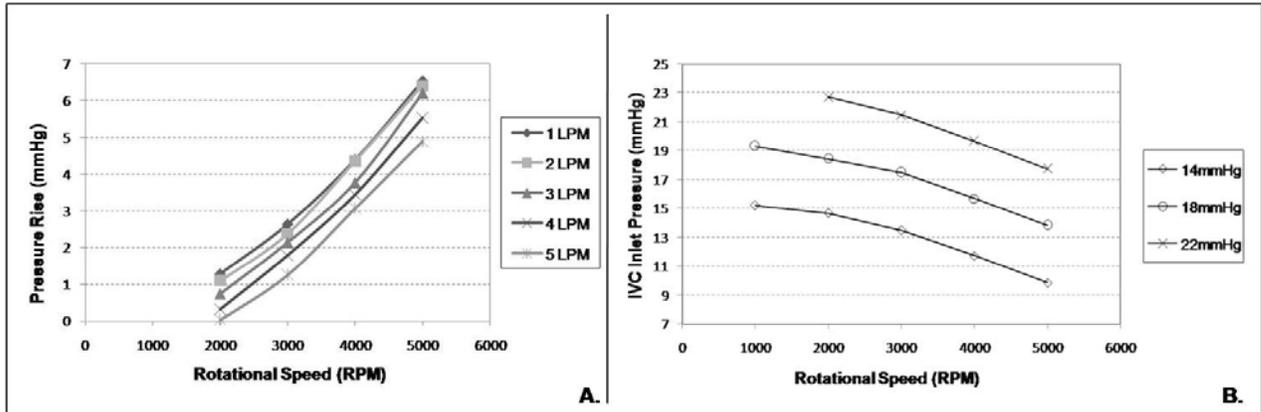
Figure 24: Pressure rise across the axial blood pump in the patient specific TCPC model and the IVC pressure as a function of increasing rotational speed. (A) Pressure rise across the pump to increases with increasing rotational speeds, as would be expected. Pulmonary arterial pressures were set to 14mmHg for these comparisons. (B) This graph shows the impact of the blood pump on the IVC pressure on the inlet side of the pump as a function of increasing rotational speed and pulmonary arterial pressures at a blood flow rate of 5 LPM.

4.2.2 Flow Profile

Careful analysis of flow fields are critical to the development of a axial flow pump designed for augmentation of the cardiovascular system. Irregular flow patterns such as vortices, eddies, and flow stagnation could increase blood exposure to high levels of shear stress activating thrombolytic factors or erythrocyte hemolysis. Figure 25 below illustrates the flow profiles for the axial flow blood pump with and without diffuser blades. The streamlines for both pump models were generated at a fluid flow rate of 3.5 LPM and pump rotational speeds of 5000 RPM. The inclusion of the diffuser blades accomplished a reduction in swirling and vortices at the pump outlet, but did not complete eliminate the irregular flow. Additionally the streamlines of the pump model with a diffuser exhibit

lower particle velocities at the outlet as compared to the pump model without a diffuser, indicating a reduction in fluid velocity and thus an increase in pressure as confirmed in the previous section.
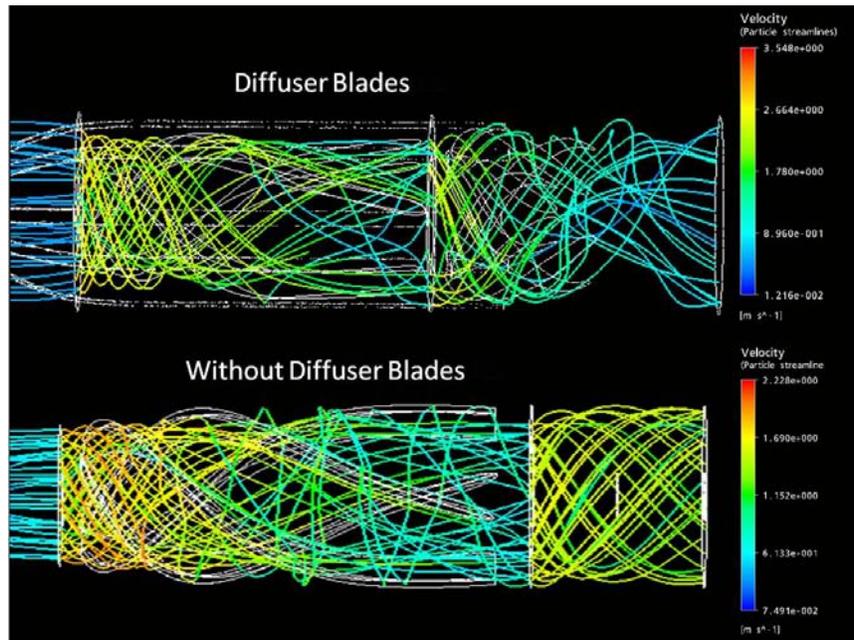
Figure 25: Reduction in Vorticity due to diffuser blades. The diffuser blades are able to redirect flow at the outlet and reduce the outflow vorticity, however not able to eliminate the flow swirl as intended.

Fluid streamlines through the idealized TCPC are displayed in Figure 26 and anatomical patient specific TCPC model 1 with and without the intravascular blood pump are displayed in Figure 27**.** The fluid streamlines correspond to operating conditions of pulmonary pressures of 14 mmHg, blood flow rate of 3.5 LPM, and pump rotational speed of 5000 RPM. Strong rotational flows were found at the outlet of both pump models, dissipating some through the pulmonary arteries.
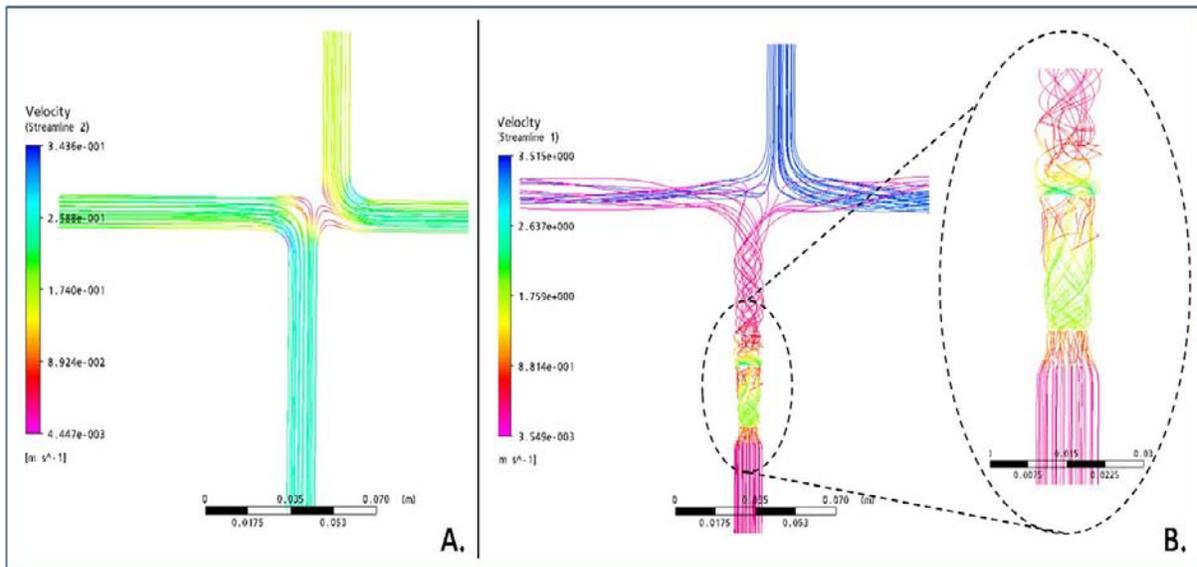
Figure 26: Fluid streamlines for the idealized TCPC model with and without the intravascular pump. Idealized model streamlines without pump (A) display high velocity turns at the outer boundaries of caval veins and pulmonary arteries connection points. (B) Velocity increases at IVC outlet due to axial flow pump.
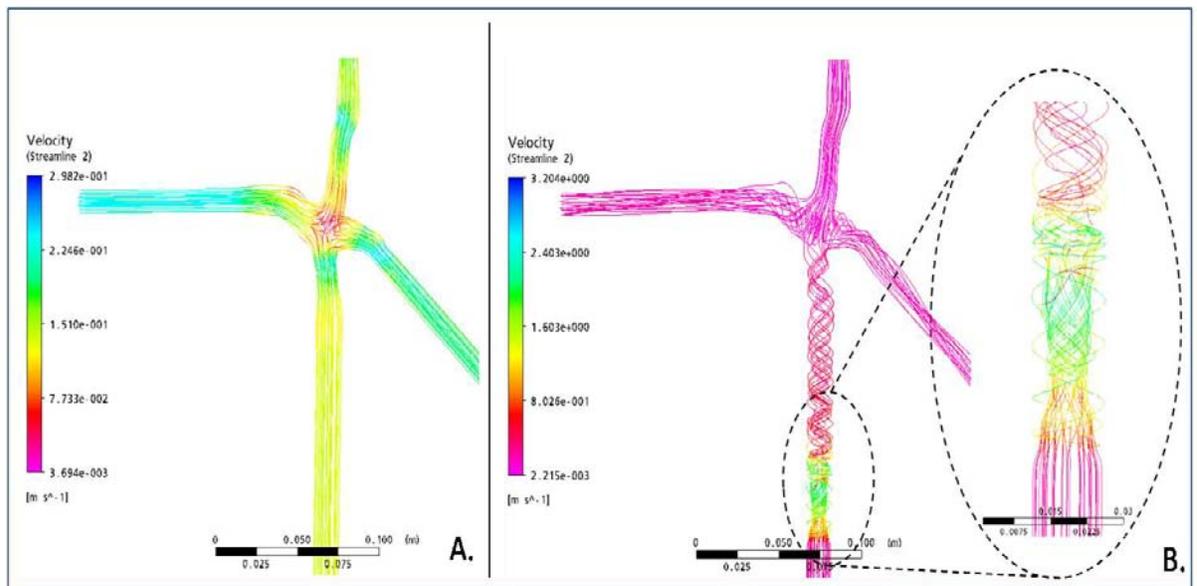
Figure 27: (A) Fluid streamlines for patient specific TCPC model without the intravascular blood pump. Lowest fluid velocities are observed at the inner boundaries of the TCPC. (B) Increased fluid particle velocities observed due to axial flow blood pump.

4.2.3 Scalar Stress Distributions

Scalar Stress represents a calculated weighted average of the shear and normal stresses and is useful for determining the level of blood trauma during pump operation. Figure 28 displays the scalar stress distribution through the intravascular cavopulmonary pump model along the rotor hub. At the design point, the highest fluid stresses of 125 Pa were estimated to exist along a small regional surface area at the leading edge of the impeller blades and more substantially along the impeller blade tips.
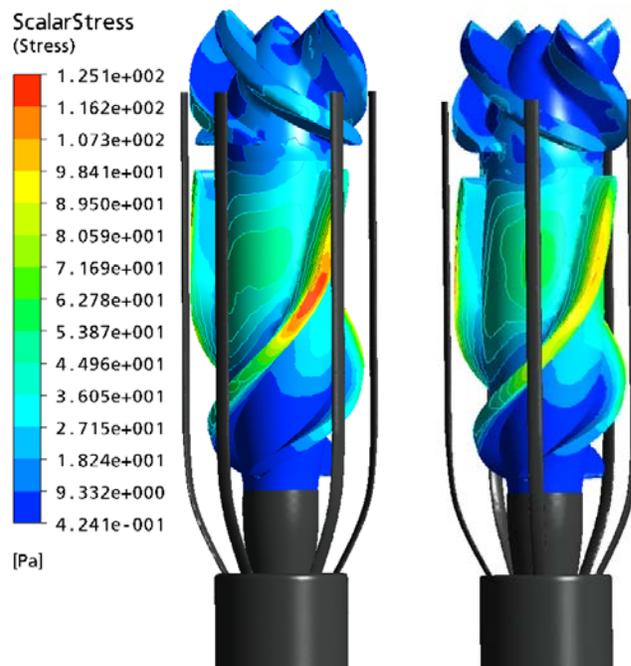
Figure 28: Scalar stress estimations on the impeller and diffuser hub surfaces. The magnitude of the scalar stress remained below 125 Pa with the highest stress regions along the impeller blade tip surface. Higher stresses were predicted at the blade tip when in closer proximity to the protective cage filaments.

Similarly, Figure 29 illustrates the scalar stress levels along the surfaces of the protective cage of filaments. The magnitude of the scalar stress remained below 120 Pa with the highest stress regions in closer proximity to impeller blade tips. These regions of high scalar stress are attributed to the interaction between the impeller blade and cage filaments.
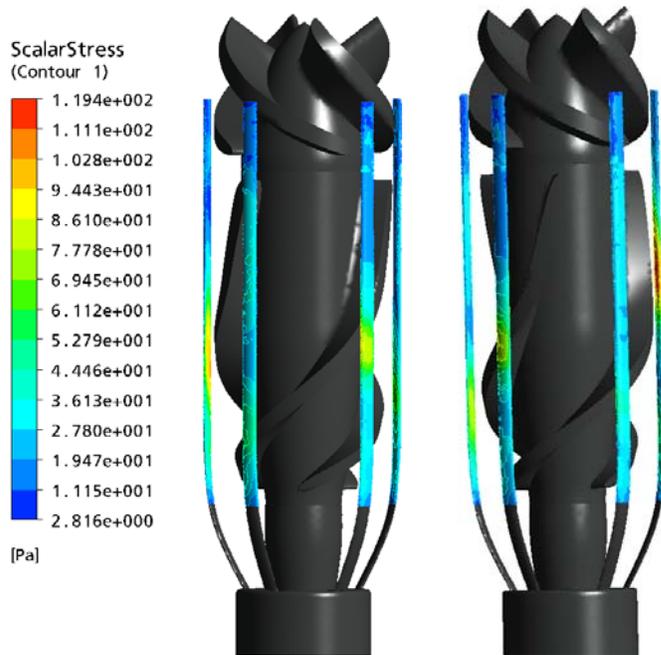
Figure 29: Scalar stress estimations on the cage filament surfaces. The magnitude of the scalar stress remained below 120 *Pa* with the highest stress regions of closer proximity to impeller blade tips.

4.2.4 Blood Viscosity Effects

In consideration of the target patient population and their varying blood viscosity values, Figure 30 illustrates the results of the viscosity study performed on the Idealized TCPC model and the impact on pump performance. It was determined that IVC pressure varied little for higher viscosity values at lower rotational speeds. This sensitivity appeared to increase to approximately 8.5% at 5000 RPM. The pressure rise across the pump was also not sensitive to increasing viscosity values at all rotational speeds with a deviation averaging 4.6%.
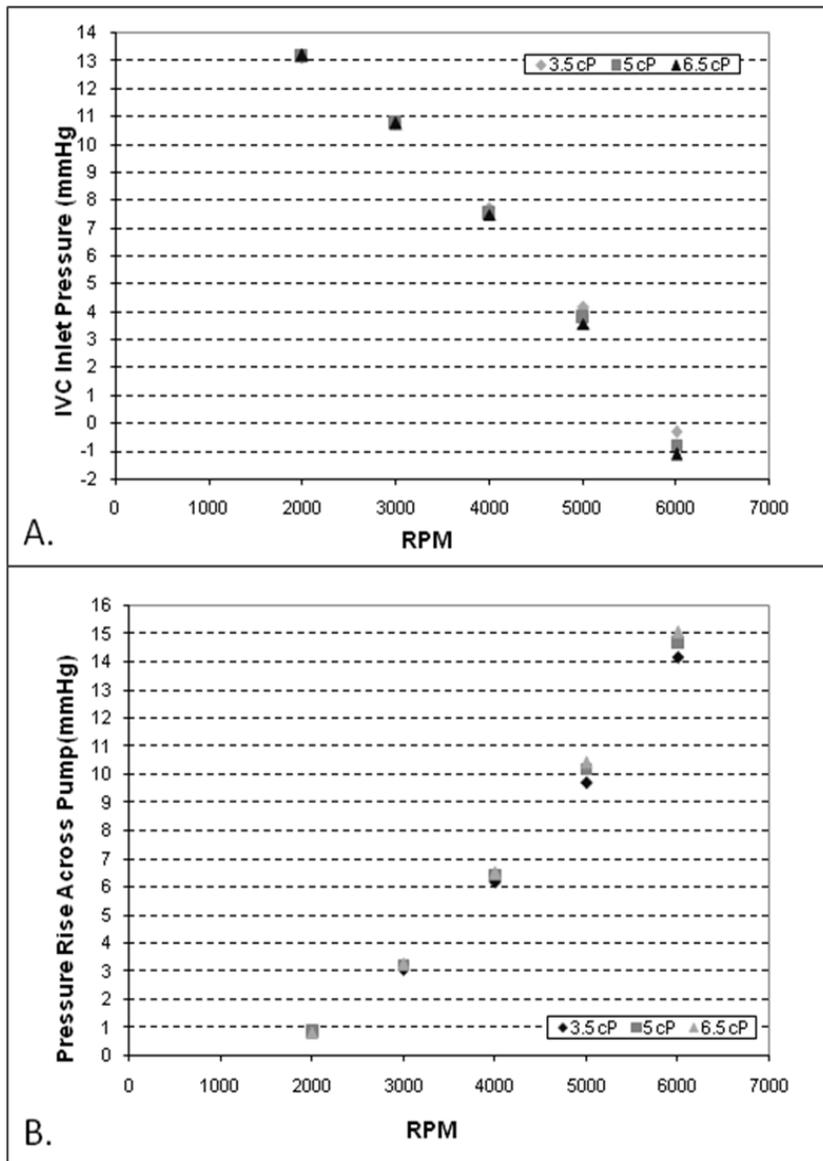
Figure 30: Effect of Blood Viscosity on Pressure in the IVC and Pressure Rise across the Pump as a function of pump rotational speed. (A) Adjustments to IVC pressure due to the pump rotational speeds varied little for higher fluid viscosity values, indicating the versatility of the pump to accommodate a range of possible patient conditions. (B) Pressure rise across the pump was maintained over all rotational speeds without reduction or measurable change due to increasing viscosity.

4.2.5 Quasi-Steady State Study

In order to detect the optimal axial rotational orientation of the impeller and diffuser blades a quasi-steady state study was performed for the cavopulmonary blood pump. Figure 31 illustrates the computational predictions from the quasi-steady analysis of the diffuser blades and their impact on pressure generation as a function of rotation position. Thirty simulations were completed for rotational increments of 3 degree. This study was performed at 5000 RPM and 2 LPM. According to the numerical findings, the

diffuser blades having a rotational position of 12 degree produced the largest pressure generation across the pump. The predicted improvement in pressure rise was found to be 6%. The diffuser blades having a rotational position of 57 degree generated the lowest pressure across the blood pump. A pressure reduction at the 57 degree position was found as compared to all other rotational positions. In comparison of the pressure generation at the initial design position at 0 degree (10 mmHg), the 57 degree rotation of the diffuser blades resulted in a pressure generation decrease of 37% (6.3 mmHg).
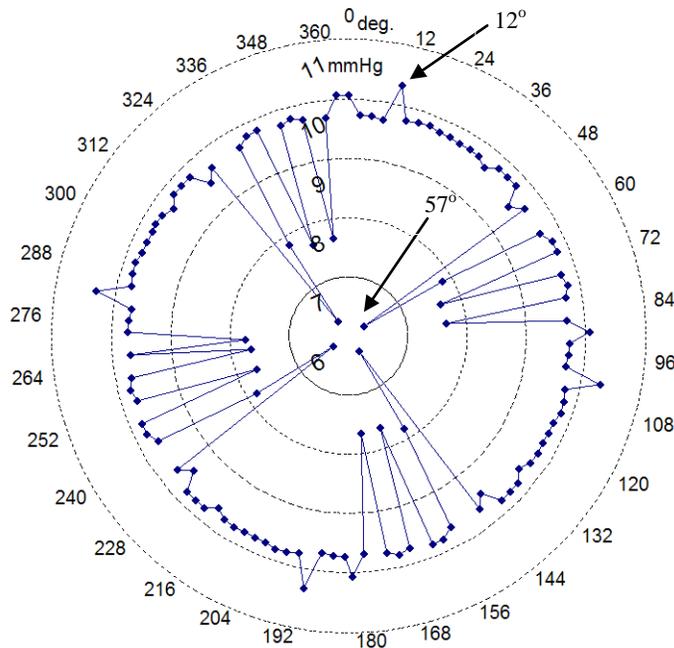
Figure 31: Quasi-steady study of the rotational impact for the diffuser blades. This study was performed at 5000 RPM and 2 LPM. The diffuser blades having a rotational position of 12 degree produced the largest pressure generation across the pump. The diffuser blades having a rotational position of 57 degree generated the lowest pressure across the blood pump.

4.2.6 Blood Damage Analysis

In addition to the quasi-steady study, a blood damage analysis was conducted to consider the potential for hemolysis from blood contacting the pump. This approach releases massless, inert particles at the inlet and tracks using streamlines their exposure time to fluid stresses. It uses a power law relationship between the scalar stress values and the exposure time to estimate an accumulated blood damage index for each particle. The blood damage analysis was completed on the idealized TCPC model to approximate the level hemolytic and thrombotic factors incurred due to blood contact with the intravascular

blood pump. Figure 32 displays the results of the numerical blood damage analysis. Three cases with a pump flow rate of 3.5 L/min were considered in this analysis: 1) a fluid viscosity of 5 cP and rotational speed of 5000 RPM, 2) a fluid viscosity of 3.5 cP and rotational speed of 5000 RPM, and 3) a fluid viscosity of 3.5 cP and rotational speed of 4000 RPM. Table 10 lists these cases and their corresponding results, as discussed in the subsequent sections.
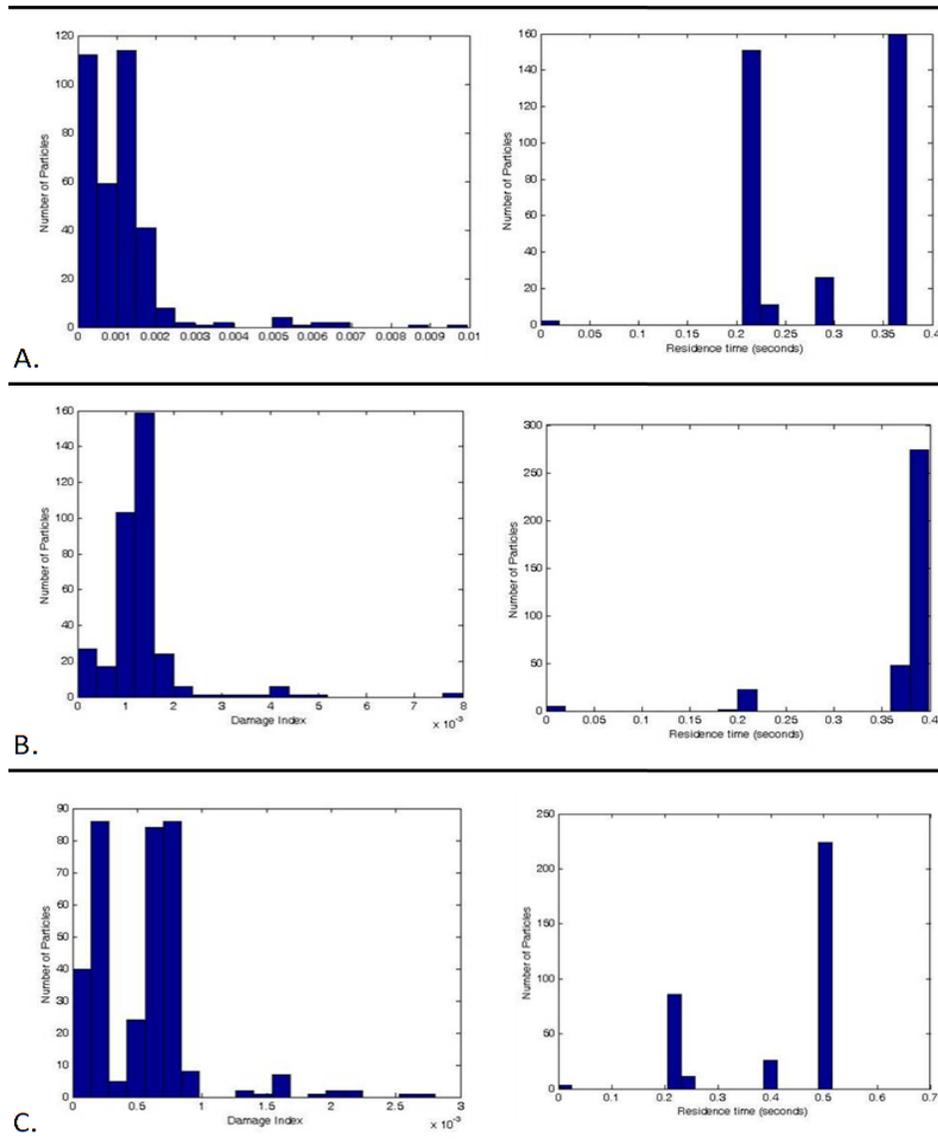
Figure 32: Blood damage indices and particle residence times for the idealized TCPC model. Intravascular blood pump operating conditions, fluid viscosities, and LPA/RPA arterial pressures as specified in Table 4. (A) Case I, (B) Case II and (C) Case III results.

Table 10: Blood damage analysis details and finding for the Intravascular Axial flow blood pump and the Idealized TCPC model.

Blood Damage Case Number	Flow Rate (LPM)	Rotational Speed (RPM)	Fluid Viscosity (cP)	Number of Particles	Mean Damage Index	Maximum Damage Index	Mean Residence Time(sec)	Maximum Residence Time(sec)
Case 1	3.5	5000	5	350	0.110%	0.990%	0.2724	0.3740
Case 2	3.5	5000	3.5	350	0.130%	0. 800%	0.3754	0.3990
Case 3	3.5	4000	3.5	350	0.0549%	0.280%	0.4222	0.5160

4.2.7 Energy Gain

In addition to the blood damage analyses, energy losses due to the cavopulmonary connection are of general concern due to associated pathophysiologies deriving from the loss of the pulmonary ventricle. A simplified control volume approach was used to calculate the hydraulic energy of the both TCPC models with and without the axial flow blood pump placed in the IVC. Figure 33 demonstrates the energy gain due to mechanical assistance of the idealized TCPC with the pump design having an impeller and diffuser blade set. These simulations occurred at an operating condition with left and right pulmonary arterial pressures of 14 *mmHg*, a fluid viscosity of 3.5 cP, a range of flow rates from 1 to 3.5 L/min, and two rotational speeds of 4000 and 5000 RPM. In comparison to the energy loss associated with the idealized TCPC without mechanical support, the predictions indicated that the use of the pump to mechanically augment pressure in the IVC increases the hydraulic energy of the TCPC as a function of both increasing rotational speed and flow rate.
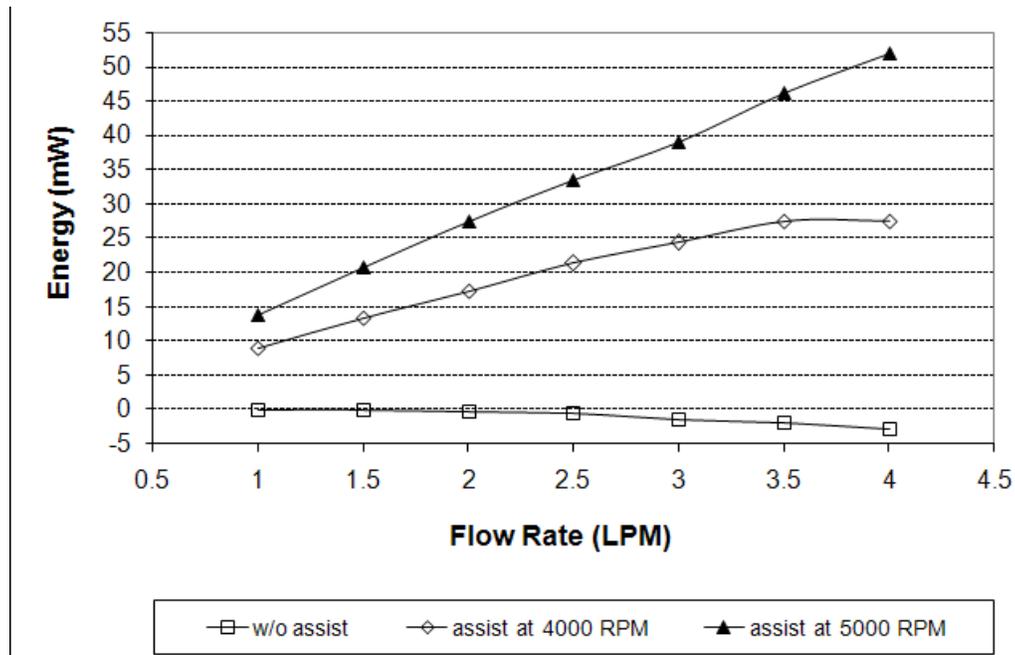
Figure 33: Energy Gain due to mechanical assistance of the idealized TCPC with a blood pump in the IVC. Mechanical assistance of the IVC pressure enhanced the hydraulic energy within the TCPC as compared to conditions without pump support.

Figure 34 demonstrates the energy gained due to mechanical assistance with the pump as compared to the energy lost due anatomy and physiology in the patient specific TCPC model. These calculations were made for the following operating conditions: left and right pulmonary arteries at 14mmHg, flow rates from 1 to 4 LPM, and pump rotation speed of 5000 RPM. As observed in the idealized energy calculations, the introduction of a circulatory assist device to the Fontan anatomy significantly increases the hydraulic energy of blood flow thus mitigating the loss from a lack of pulmonary ventricle.
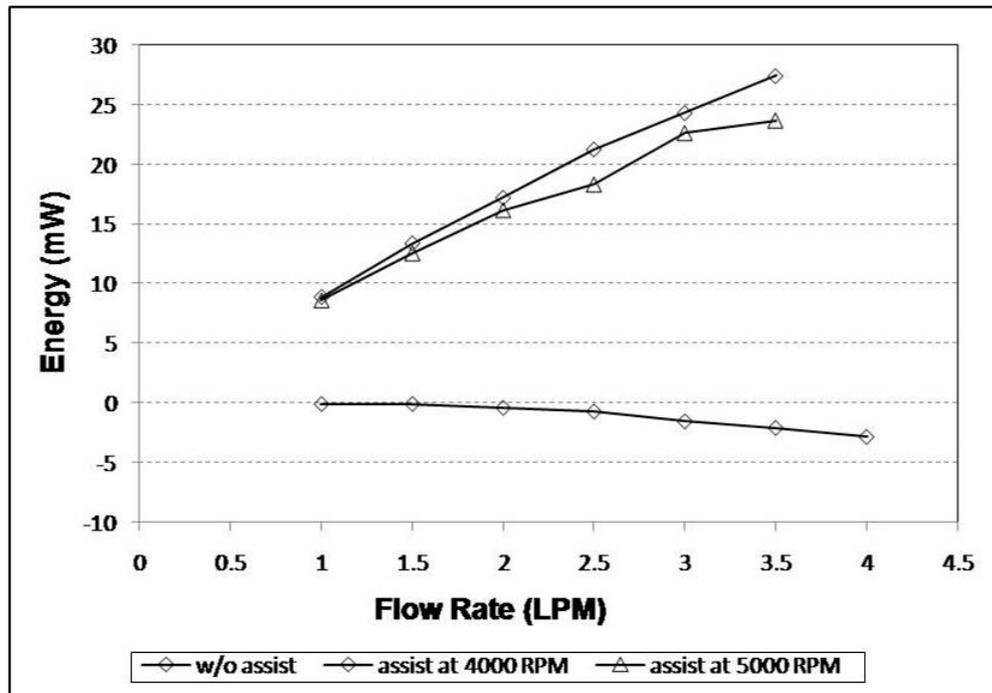
Figure 34. Energy Gain due to mechanical assistance of the patient specific TCPC with a blood pump in the IVC. Mechanical assistance of the IVC pressure enhanced the hydraulic energy within the patient specific TCPC as compared to conditions without pump support.

4.3 Chapter Summary

Based upon the results of numerical simulations of the two pump models and two extra-cardiac Fontan models, the intravascular axial flow blood pump was optimized in design as follows: an impeller with 3 counterclockwise helically wrapped blades, a diffuser region with 4 clockwise helically wrapped blades at a 12° offset to the impeller, and protective cage with 5 filaments. The optimized pump generates pressure rises of 2 to 25 mmHg for flow rates of 1 to 7.5 LPM and rotational speeds of 2000 to 8000 RPM, reduces irregular flow perturbations at the pump outlet, and demonstrates low probabilities for

erythrocyte damage. Table 11 outlines the design specifications and numerical results of the optimized intravascular, axial flow blood pump.

Table 11: Summary of Axial Flow Blood Pump Design Specifications and Results

Design Specifications and Investigations	Numerical Results
Impeller Blade Count	3
Impeller Blade Orientation	Counter-clockwise
Diffuser Blade Count	4
Diffuser Blade Orientation	Clockwise
Impeller-Diffuser Optimal Rotational Offset	12°
Axial Flow Blood Pump Pressure Generation	1 - 26 mmHg
Blood Flow Rates	1 - 7.5 LPM
Pulmonary Arterial Pressure	10 -26 mmHg
Pump Rotational Speed	1000 - 8000 RPM
Maximum Scalar Stress	125 Pa
Maximum Blood Damage Index	0.99%
Mean Blood Damage Index	0.10%
Maximum Residence Time	0.516 sec
Mean Residence Time	0.35667 sec
Maximum Energy Gain (Idealized)	45 mW
Maximum Energy Gain (Patient Specific)	27 mW

CHAPTER 5 DISCUSSION

Fontan and Baudet introduced the total right heart bypass in 1968 [86, 87]. Decades prior to their original description, at least 40 different experimental procedures to bypass the right heart provided evidence that venous pressure alone could act as the driving force for blood flow into pulmonary circulation. The current treatment paradigm for patients with univentricular physiology is a staged surgical palliation, leading to a Fontan conversion. Several modifications to the Fontan have developed over time with the TCPC providing a direct connection from the superior and inferior vena cava to the pulmonary arteries. In the absence of a pulmonary ventricle, the blood traveling through the Fontan circulation experiences a loss of energy with minimal to no pulsatility as it flows through the pulmonary circulation [1-4, 10, 11, 15, 65, 88]. Secondary pathologies due to the new "man-made" physiology include reduced preload, diminished exercise capacity, supraventricular arrhythmias, protein losing enteropathy, aortopulmonary and veno-veno collateral vessels. It has been theorized that the long-term effects of the Fontan paradox (caval hypertension and relative pulmonary hypotension) can be reversed through mechanical support [22, 49, 61].

This thesis documented the methods, materials, and results for two mechanical cardiovascular assist devices designed to augment the hemodynamics of adolescent and adult Fontan patients. A non-invasive method for circulatory support provided via

counterpulsation external pressure technology was described in Chapter 2 and the results were outlined is Chapter 4. Likewise, the minimally invasive method using an intravascular axial flow blood pump inserted into the IVC was described in Chapter 3 with numerical simulation results outlined in Chapter 4. Discussions for each method of mechanical cardiovascular assist are in the sections below.

5.1 Non-invasive External Pressure Augmentation

The goal of the non-invasive cardiovascular assist modality was to develop and design an innovative non-invasive medical device for the prevention and/or treatment of pathological implications in postoperative Fontan patients adjusting to their new "man-made" physiology. This device would provide cardiovascular assistance to patients through the augmentation of systemic blood flow to the pulmonary arteries, thus increasing venous return and pulmonary perfusion, and reducing cardiac afterload. The device operates through the medium of external pressure application to the lower limbs and abdomen, forcing forward propulsion of blood towards the heart and pulmonary circulation, analogous to muscular contractions during exercise. For this thesis clinical trials were completed utilizing retrofitted MAS trousers as the channel for external pressure augmentation. Positive results from the clinical trials serve as the clinical feasibility study for development of a novel external cardiovascular assist device for patient use at home. Subject recruitment began immediately after we received Virginia Commonwealth University IRB approval in January 11, 2009 (VCU IRB #HM11906).

Two patient trials were completed during the first year of the IRB approved clinical investigation. Clinical trial subject population was limited due to exclusion criteria and reduced qualified candidate pool of a unique cohort of cardiovascular defects. The first clinical trial occurred February 19, 2009 with Dr. William Moskowitz conducting the cardiac catheterization on a 37 year old female single ventricle patient with a TCPC extra-cardiac Fontan anatomy. Results indicated an increase in pressure of approximately 4 -15 mmHg for systolic and diastolic pressure measured in the aortic arch. As illustrated in Figure 14, trends in patient 1 data demonstrate almost a linear correlation with increases in external pressure application providing evidence that the application of external pressure increased venous pressures which translated to an increased of blood flow to pulmonary circulation and subsequently the aortic arch.

In contrast to patient 1, patient 2 did not demonstrate the expected linear correlation between the external pressure application and resulting influence in aortic blood pressure. Several considerations and speculations can be offered as explanation for the unexpected trends exhibited by patient 2. The second clinical trial occurred on October 6, 2009 with Dr. William Moskowitz conducting the cardiac catheterization on a 24 year old male single ventricle patient with a classical Fontan with the right atrium is preserved, also known as an intra-atrial Fontan. During the clinical trial, the abdominal section was neglected due to the patient's medical history of sleep apnea posing as exclusion criteria for any external pressure application with possible respiratory constriction affects. Hepatic vessel compliance during pressure application to the lower limbs may account for a portion of the pressure dissipation downstream of the heart. The patient's Fontan anatomy may have also

contributed to the reduced response of external pressure application due to compliance of the intact right atrium expanding to accommodate the increased volumetric blood flow. Additionally during the catheterization, observations were made with patient respirations and correlations to patient pulmonary arterial pressures. During deep sleep it was noted that the patient's inspiration and expiration had discernable affects on pulmonary arterial pressures, thus insinuating observed pressure augmentation to aortic blood pressure may not be independent of respiratory cycle.

5.2 Minimally Invasive Intravascular Blood Pump

In support of the development of a minimally invasive cavopulmonary assist device, this thesis outlined the results of numerical analyses on an intravascular blood pump placed in Fontan TCPC models. The mechanical circulatory device is a collapsible, percutaneously inserted, axial flow blood pump designed to function as a bridge-to-transplant or bridge-to-recovery for adult Fontan patients. Description and placement of the pump can be found in Figures 9 with a full detail presented in previous chapters.

Extensive numerical studies were conducted to test pump performance in an idealized TCPC model and a patient specific TCPC model. Left and right pulmonary arterial pressures were examined at five pressure points from 10 *mmHg* to 26 *mmHg*, blood viscosities from 3.5cP to 6.5 cP, and pump rotational speeds from 1000 RPM to 8000 RPM. The pump demonstrated hydraulic performance as quantified by pressure generations of 1 to 25 mmHg over flow rates of 1 to 7.5 LPM. This range of pressure rises

and flow rates is sufficient to support an adolescent and adult Fontan patient. Hydraulic performance curves were characteristically consistent for varying rotational speeds.

Fluid viscosity influences were found to be minimal with greater effects found at higher rotational speeds as demonstrated in Figure 30 in chapter 4. The low influence of higher fluid viscosities on pump performance is important since a majority of Fontan patients are polycythemic, thus having a wide range of blood hematocrits. A versatile pump design that is not subject to performance losses over a range of blood hematocrits is advantageous for Fontan patients.

Blood damage analyses were performed on three cases, all of which resulted in a maximum damage index of less than 1% and maximum residence time of less than 0.52 seconds indicating a low probability of blood damage due to interaction with the pump. Two cases were performed off design point of the pump reflecting the position that the pump will often function off ideal design parameters. The majority of tracked particles indicated an even lower probability of damage as demonstrated in Figure 32 and Table 10 in Chapter 4. The maximum blood damage indices also predict a very low N.I.H for these operating conditions examined. Blood pumps are designed to maintain an N.I.H level below 0.005 g/100L for clinical use. The predicted N.I.H values remained one to two orders of magnitude lower than the cutoff limit for clinical use. Table 12 below outlines the results from the blood damage analyses as compared to selected clinically available adult rotary blood pumps. Estimations indicate that centrifugal blood pumps have damage indices of 4% to 6% [79] and axial blood pumps have higher indices, ranging from 19% to 40% [61]. Based on this comparison and the number of particles used in this study, these

results suggest that a majority of the tracked particles have a low probability of damage,
however blood bag experimentation must be performed to quantify the levels of hemolysis
for this intravascular blood pump.

Table 12: The comparison of blood damage indices and N.I.H values for selected adult rotary blood pumps.[51, 61, 89-92]

Pump	Type	N.I.H. (g/100L)	Damage Index (%)
Valvo Pump	Axial	0.030	200
MicroMed-DeBakey	Axial	0.0028	19
Biomedicus BP-80	Centrifugal	0.0007	5
Berlin Incor I	Axial	0.006	40
HeartMate II	Axial	0.005	33
Intravascular Pump*	**Axial**	**---**	**1**

To analyze the interactive dynamics between the pump and the TCPC, we
calculated the energy of the total system using a simplified control volume approach. This
technique has been commonly used by researchers and clinicians to maximize surgical
optimization of the TCPC and elucidate new surgical strategies to mitigate hydraulic
energy losses [65]. Under conditions where no artificial right ventricle or subpulmonary
power source exists, such as those present in the Fontan physiology, energy losses
invariably occur with blood flow in the TCPC and subsequent flow into the LPA and RPA.
Previous studies found the energy losses (i.e. power loss) in the TCPC to increase due to
higher flow rates, lower limb exercise, dramatic changes in the geometry of the
anatosmoses, and lack of caval offset [93]. By incorporating a blood pump into the IVC,
energy augmentation is observed, rather than hydraulic losses. This positive augmentation
of energy due to the pump in the IVC is the intended result and may translate into an
improvement in venous return and cardiac output for Fontan patients. In conjunction with

surgical optimization of the TCPC, the introduction of periodic or short-term

cavopulmonary assist may serve as a viable, long-term, clinical management strategy for

Fontan patients.

Figure 33 in Chapter 4 illustrates the energy losses of the idealized TCPC without a

pump in the IVC in comparison to the energy gains of the idealized TCPC with the

intravascular pump (impeller and diffuser blade set) in the IVC. Pump rotational speeds of

4000 RPM and 5000 RPM were examined to determine the energy augmentation in the

idealized TCPC. A steady increase in energy as a function of flow is observed from 1 to

3.5 L/min for the 4000 RPM operating conditions. Upon reaching 4 L/min, the energy

performance curve at 4000 RPM ceases to increase in slope; the inherent hydraulic losses

from this higher flow rate through the idealized TCPC and the lower head produced by the

pump begin to inhibit energy augmentation. For the 5000 RPM operating condition, the

pump is able to continuously improve energy gains over the entire 1 to 4 L/min flow range.

Similar trends were observed for the patient specific TCPC Fontan model. The energy gain

from the pump in the patient specific TCPC model peaked under 30mV with similar linear

trends indicating that increase in flow rates at give pump RPM would result in increased

energy gain.

In examining the outflow conditions of the pump, a rotational component of the

flow was predicted by the computational analysis. The introduction of a diffuser region

consisting of a hub with 4 clockwise helically wrapped blades demonstrated a reduction in

vorticity at the outlet of the pump as compared to previous models without a diffuser

region. Figure 25 illustrates the diminution of rotational fluid flow at the outlet region of

the pump. Complete elimination of irregular flow patterns were not achieved thereby requiring the above discussed analyses of energy gain and blood damage indices. Despite the rotational flow component, power or energy enhancement was achieved, and low blood damage indices were predicted. Additional design work will be performed to minimize this flow rotational and straighten the blood flow leaving the pump.

CHAPTER 6 FUTURE WORK AND CONCLUSIONS

6.1 Limitations and Future Work

Previous chapters discussed two novel approaches for the development of mechanical circulatory devices for Fontan patients. A non-invasive method using external pressure augmentation to the lower limbs demonstrated notable increases in systolic and diastolic blood pressures for in two patients. A minimally invasive method using a percutaneously inserted, intravascular blood pump computationally demonstrated acceptable pressure generations to augment the Failing Fontan hemodynamic. Both modalities show promise in the clinical support and treatment of Fontan patients: the pressure pants as long-term preventative support and axial flow blood pump for short term bridge support. Study limitations are discussed in this chapter along with issues to be addressed in future work.

6.1.1 Pressure Garment

A considerable limitation to thesis work with regard to the pressure garment clinical trials was the lack of test subject population. During the year and a half time frame of the VCU IRB approved clinical trials, only two patients successfully met the criteria and participated in the study. Factors influencing the deficiency in subject population include the diminutive single ventricle Fontan cohort perpetuated by a single intuitional investigation and extensive exclusion criteria inclusive of several secondary pathological

conditions common to Fontan patients. Future clinical studies for continued development of the pressure garment will address these limitations by seeking multi-institutional clinical trials.

During development of the clinical external pressure augmentation protocol several inflation/deflation intervals and timings were considered. Interval cycles excogitated for the clinical trial included cardiac cycle synchronization, respiratory cycle synchronization and constant interval based. Research indicates that the majority of clinical external pressure pulsation devices are synchronized to the patient's cardiac cycle thus requiring more advanced technology and a nurse or technician to monitor and operate the device for proper synchronization. Having stated our predispositions of EECP delivery with accordance to synchronization protocol in Chapter 2, it was inferred that counterpulsasive therapy less synchronization will also demonstrate beneficial results. This assumption was strongly supported by the results this study in addition to the reviewed literature. Discrepancies arise, however, when attempting to decipher the degree of assistance provided by counterpulsation administered at a basal rate unlinked to a patient's cardiac cycle. If future work includes investigation of cardiac synchronization, it is expected that cardiac synchronization is significant to the level of augmentation provided by counterpulsation, however the occurrence of such augmentation is independent of synchronization.

Respiratory cycle synchronization was also considered. Chest wall expansion during inhalation and subsequent depression during exhalation influence cardiac filling and ejection. Upon deep inhalation, the second heart sound can split providing audible

evidence of a delay between the closing of the pulmonary and aortic valves. Though respiratory synchronization effects would have been interesting to investigate, it was not included due to the overall goal of developing a therapeutic device for patients to use at home, thus requiring a simpler model. However, due to correlating respiration cycle and pulmonary arterial pressures observations made during the second patient's clinical trial, continued development of an external mechanical cardiac assist device would include respiratory cycle synchronization analyses.

Based upon the need for a simple device designed to augment venous flow a constant interval cycle was determined to be the favorable timing for pressure garment inflation and deflation. The constant interval cycle was conducted as a square wave, with inflation demonstrated as the highpoint when the pressure is applied and deflation as the lowpoint when the pressure is removed. An ideal square wave interval cycle would demonstrate precision in holding the pressure at a specific target and instantaneous inflation and deflation. Though based on the ideal, the clinical trial conducted with retrofitted medical anti-shock trousers resembled more of a trapezoidal wave with sloping increases and decreases in pressure during cycles. Additionally, during the inflation hold periods loss of pressure may be exhibited do to leaks within the pressure pant system. With these limitations considered, it was determined that for the purpose of augmenting venous blood flow to the heart, slight fluctuations in external pressure are inconsequential and thus do not contravene the use of a constant interval cycle nor discount the integrity of trial results. However future work with the pressure garment will not only reconsider the before

mentioned synchronization affects but also reduce pressure loses during inflation holds by identifying and subsequently rectifying system leaks.

The VCU/MCV catheterization laboratory employs SIEMENS (Siemens Corporation, New York, NY) technology. The current software package conducts real-time analyses and stores user defined values or pressure waveform moments at a defined time. Continual recording of pressures for analysis at a later time is outside the software capabilities thus limiting the view of external pressure augmentation influence on patient hemodynamics. Additionally, the software is confined to output averaged pressures for selected waves and incapable of outputting discrete data, greatly influencing the accuracy of data analyses.

6.1.2 Intravascular Blood Pump

This thesis work on the intravascular blood pump has a number of limitations that must be addressed during the next stage of development. The boundary conditions as specified are for steady flow analyses; transient flow simulations and fluid structure interaction (FSI) studies with varying inlet and outlet impedances, vessel compliance, and lung compliance would provide more accurate information about the interactive dynamics between the physiology and the blood pump. A detailed turbulence model study would also generate valuable insight into the fluid dynamics.

The manufacturing of three-dimensional models of the idealized Fontan TCPC anatomy and patient specific TCPC anatomy with inclusion of the pump prototype in the IVC is currently underway. These models will allow for laser flow measurements and

hydraulic performance testing to take place and to validate numerical predictions from this thesis.

The blood damage analyses conducted with the idealized TCPC model did not consider heat transfer, platelet activation, and transient effects in the fluid stresses due to blade rotation. Additionally, the blood damage analysis uses a power law equation generating overestimations in the levels of hemolysis. The overestimation, however, allows pump design to err on the side of caution. Hemolysis testing using physical prototypes would provide more realistic confirmation of actual trauma levels.

6.2 Conclusions from Research

This thesis presented two novel approaches for the development of a mechanical cardiovascular assist device for patients with Fontan physiology. The first approach suggested the design of a noninvasive mechanical device which would augment Fontan hemodynamics via external pressure application to the lower limbs and abdomen. This thesis presented the results of a VCU IRB approved clinical trial for feasibility studies and provided proof of concept for the design of a novel pressure garment. The pressure garment is intended for patient use at home at their convenience to alleviate cardiac workload providing hemodynamic relief. Results from patient trials indicate external application to the lower limbs and abdomen of as little as 10 mmHg below baseline diastolic may be enough to augment Fontan pressures and improve hemodynamics functioning in a preventative and sustaining manner.

The second approach involved the design of a minimally invasive, percutaneously inserted, intravascular blood pump design for placement in the IVC. This collapsible axial flow blood pump is designed with a 3-bladed impeller, 4-bladed diffuser, and radially arranged cage filaments serving as touchdown surfaces to protect the vessel wall from rotating components. This thesis presented the numerical analyses of the interactive fluid dynamics between the cavopulmonary connection and a mechanical blood pump. The pump would serve as a bridge-to-transplant, bridge-to-recovery, or bridge-to-surgical reconstruction. A pressure augmentation of as little as 2 to 5 mmHg may be sufficient to stabilize and reverse hemodynamic deterioration in Fontan patients. Computational predictions indicate the blood pump would augment pressure acceptably in both the idealized TCPC and patient specific TCPC models and result in a hydraulic energy boost or gain for a range of viscosity values, LPA and RPA pressures, flow rates, and pump rotational speeds. These results support the continued design and development of this cavopulmonary assist device, building upon previous numerical work and future experimental testing.

Both modalities that were evaluated in this thesis project showed tremendous promise to potentially support Fontan patients in the acute and long-term clinical setting. The designs of both modalities will evolve over time, ultimately leading to two viable therapeutic options for Fontan patients and addressing a significant human health problem.

Literature Cited

+

Literature Cited

1.   Tanner, K., N. Sabrine, and C. Wren, *Cardiovascular malformations among preterm infants.* Pediatrics, 2005. **116**(6): p. e833-8.

2.   Wren, C., Z. Reinhardt, and K. Khawaja, *Twenty-year trends in diagnosis of life-threatening neonatal cardiovascular malformations.* Arch Dis Child Fetal Neonatal Ed, 2008. **93**(1): p. F33-5.

3.   Jayakumar, K.A., et al., *Cardiac transplantation after the Fontan or Glenn procedure.* J Am Coll Cardiol, 2004. **44**(10): p. 2065-72.

4.   Hosein, R.B., et al., *Factors influencing early and late outcome following the Fontan procedure in the current era. The 'Two Commandments'?* Eur J Cardiothorac Surg, 2007. **31**(3): p. 344-52; discussion 353.

5.   Christianson, A., C.P. Howson, B. Modell, *March of Dimes Global Report on Birth Defects: The Hidden Toll of Dying and Disabled Children*. 2006, March of Dimes Birth Defects Foundation: White Plains, NY.

6.   Dove, S. *Descriptions of Congenital Heart Defects*. March 27, 2010 [cited 2010.

7.   Pavan, M., et al., *ALDH1A2 (RALDH2) genetic variation in human congenital heart disease.* BMC Med Genet, 2009. **10**: p. 113.

8.   Warnes, C.A., et al., *ACC/AHA 2008 Guidelines for the Management of Adults with Congenital Heart Disease: Executive Summary: a report of the American College of Cardiology/American Heart Association Task Force on Practice Guidelines (writing committee to develop guidelines for the management of adults with congenital heart disease).* Circulation, 2008. **118**(23): p. 2395-451.

9.   Valdes-Dapena, M. and E. Gilbert-Barness, *Cardiovascular causes for sudden infant death.* Pediatr Pathol Mol Med, 2002. **21**(2): p. 195-211.

10. Hirsch, J.C., et al., *Fontan operation in the current era: a 15-year single institution experience.* Ann Surg, 2008. **248**(3): p. 402-10.

11. Ashburn, D.A., et al., *Outcomes after the Norwood operation in neonates with critical aortic stenosis or aortic valve atresia.* J Thorac Cardiovasc Surg, 2003. **125**(5): p. 1070-82.

12. De Leval, M.R., *The Fontan Circulation: A challenge to William Harvery?* Nature Clinical Practice Cardiovascular Medicine, 2005. **2**: p. 202 -208.

13. de Leval, M.R., *The Fontan circulation: What have we learned? What to expect?* Pediatr Cardiol, 1998. **19**(4): p. 316-20.

14. Kayatas, M., et al., *Comparison of the non-invasive methods estimating dry weight in hemodialysis patients.* Ren Fail, 2006. **28**(3): p. 217-22.

15. Leyvi, G., H.L. Bennett, and J.D. Wasnick, *Pulmonary artery flow patterns after the Fontan procedure are predictive of postoperative complications.* J Cardiothorac Vasc Anesth, 2009. **23**(1): p. 54-61.

16. Bacha, E.A., et al., *Connection of discontinuous pulmonary arteries in patients with a superior or total cavopulmonary circulation.* Ann Thorac Surg, 2008. **86**(6): p. 1948-54.

17. Gentles, T.L., et al., *Fontan operation in five hundred consecutive patients: factors influencing early and late outcome.* J Thorac Cardiovasc Surg, 1997. **114**(3): p. 376-91.

18. Mahle, W.T., et al., *Impact of early ventricular unloading on exercise performance in preadolescents with single ventricle Fontan physiology.* J Am Coll Cardiol, 1999. **34**(5): p. 1637-43.

19. West, J.B., C.T. Dollery, and A. Naimark, *DISTRIBUTION OF BLOOD FLOW IN ISOLATED LUNG; RELATION TO VASCULAR AND ALVEOLAR PRESSURES.* J Appl Physiol, 1964. **19**: p. 713-24.

20. Lamour, J.M., K.R. Kanter, D.C. Naftel, M.R. Chrisant, W.R. Morrow, B.S. Clemson, J.K. Kirklin, *The Effect of Age, Diagnosis, and Previous Surgery in Children and Adults Undergoing Heart Transplantation for Congenital Heart Disease.* J Am Coll Cardiol, 2009. **54**(2): p. 160-165.

21. Petko, M.R.J.M., G. Wernovksy, et al., *Surgical Reinterventison following the Fontan Procedure.* Pediatric Anaesth, 2003(18): p. 320-324

22.   Rodefeld, M., J.H. Boyd, B.J LaLone, et al., *Cavopulmonary assist: Circulatory support for the univerntricular Fontan circulation.* Cardiol Young, 2003(16): p. 55-60.

23.   Sadeghi, A.M., et al., *Short-term bridge to transplant using the BVS 5000 in a 22-kg child.* Ann Thorac Surg, 2000. **70**(6): p. 2151-3.

24.   Senzaki, H., et al., *Cardiac rest and reserve function in patients with Fontan circulation.* J Am Coll Cardiol, 2006. **47**(12): p. 2528-35.

25.   Throckmorton A.L., J.K., D. Madduri, *Mechanical axial flow blood pump to support the cavopulmonary circulation.* Int J Artif Organs, 2008(31): p. 970-982.

26.   Throckmorton, A.L., S.G. Chopski, *Pediatric circulatory support systems: current strategies and future directions. Biventricular and univentricular mechanical assistance.* ASAIO J, 2008(54): p. 491-497.

27.   Russo, P., et al., *Use of a ventricular assist device as a bridge to transplantation in a patient with single ventricle physiology and total cavopulmonary anastomosis.* Paediatr Anaesth, 2008. **18**(4): p. 320-4.

28.   Throckmorton, A.L., et al., *Pediatric circulatory support systems.* ASAIO J, 2002. **48**(3): p. 216-21.

29.   Bartlett, R.H., *Extracoporeal life support: History and new directions.* Semin Perinatol, 2005. **29**: p. 2-7.

30.   Suzuki, Y., et al., *Extracorporeal membrane oxygenation circulatory support after congenital cardiac surgery.* ASAIO J, 2009. **55**(1): p. 53-7.

31.   Fynn-Thompson, F., C. Almond, *Pediartric ventricular assist devices.* Pediatr Cardiol, 2007. **28**: p. 149-155.

32.   Haines, N.M., et al., *Extracorporeal Life Support Registry Report 2008: neonatal and pediatric cardiac cases.* ASAIO J, 2009. **55**(1): p. 111-6.

33.   Hannan, R.L., J.W. Ojito, M.A. Ybarra, et al., *Rapid cardiopulmonary support in children with heart disease: A nine year experience.* Ann Thorac Surg, 2006. **82**: p. 1637-1642.

34.   Duncan, B.W., *Mechanical cardiac support in the young. Short-term support: ECMO.* Semin Thorac Cardiovasc Surg Pediatr Card Surg Annu, 2006: p. 75-82.

35.   Cooper, D.S., et al., *Cardiac extracorporeal life support: state of the art in 2007.* Cardiol Young, 2007. **17 Suppl 2**: p. 104-15.

36.   Potapov, E.V., B. Stiller, and R. Hetzer, *Ventricular assist devices in children: current achievements and future perspectives.* Pediatr Transplant, 2007. **11**(3): p. 241-55.

37.   Conrad, S.A., P.T. Rycus, H. Dalton, *Extracorporeal life support registry report.* ASAIO J, 2004. **51**: p. 4-10.

38.   Ravishankar, C., J.W. Gaynor, *Mechanical Support of the Functionally Single Ventricle.* Cardiol Young, 2006(16): p. 55-60.

39.   Ungerleider, R., I. Shen, T. Yeh, et al., *Routine Mechanical Ventricular Assist Following the Norwood Procedure-Improved Neurologic Outcome and Excellent Hospital Survival.* Ann Thorac Surg, 2004(77): p. 18-22.

40.   Rogers, A., A. Trento, R.D. Siewers, B.P. Griffith, R.L. Hardesty, E. Pahl, L.B. Beerman, R.J. Fricker, D.R. Fischer, *Extracoporeal Membrane Oxygenation for Postcardiotomy Cardiogenic Shock in Children.* Ann Thorac Surg, 1989(47): p. 903-906.

41.   Chatzis, A.C., G.A.J. Tsoutsinos, P.N. Zavaropoulos, G.V. Kirvassillis, et al., *Extracoporeal membrance oxygenation circulatory support after cardiac surgery.* Transplant Proc, 2004. **36**: p. 1763-1765.

42.   Chaturvedi, R.R., D. Macrae, K.L. Brown, et al., *Cardiac ECMO for biventricular hearts after paediatric open heart surgery.* Heart, 2004. **90**: p. 545-551.

43.   Ziomek, S., J.E. Harrell, J.W. Fasules, S.C. Faulkner, C.W. Chipman, M. Moss, et al., *Extracorporeal Membrane Oxygenation for Cardiac Failure After Congenital Heart Operation.* Ann Thorac Surg, 1992(54): p. 861-868.

44.   Pennington, G., M.T. Swartz, *Circulatory Support in Infants and Children.* Ann Thorac Surg, 1993(35): p. 233-237.

45.   Dalton, H., P.T. Rycus, S.A. Conard, *Update on extracoporeal life support.* Semin Perinatol, 2005. **29**: p. 24-33.

46.   Duncan, B.W., *Mechanical circulatory support for infants and children with cardiac disease.* Ann Thorac Surg, 2002. **73**: p. 1670-1677.

47.   Chohen, G., L. Permut, *Decision making for mechanical cardiac assist in pediatric cardiac surgery.* Semin Thorac Cardiovasc Surg, 2005. **8**: p. 41-50.

48.   Ricci, M., et al., *Initial experience with the TandemHeart circulatory support system in children.* ASAIO J, 2008. **54**(5): p. 542-5.

49.   Throckmorton A.L., J.Y.K., S.G. Chopski, S.S. Bhavsar, W.B. Moskowitz, S.D. Gullquist, J.J. Gangemi, C.M. Haggerty, A.P. Yoganathan, *Mechanical Cavopulmonary Assist using an Intravascular Axial Flow Blood Pump.* Ann Thorac Surg, Under Review.

50.   Riemer, R.K., et al., *Mechanical support of total cavopulmonary connection with an axial flow pump.* J Thorac Cardiovasc Surg, 2005. **130**(2): p. 351-4.

51.   Cardarelli, M.G., et al., *Berlin heart as a bridge to recovery for a failing Fontan.* Ann Thorac Surg, 2009. **87**(3): p. 943-6.

52.   Frazier, O.H., I.D. Gregoric, and G.N. Messner, *Total circulatory support with an LVAD in an adolescent with a previous Fontan procedure.* Tex Heart Inst J, 2005. **32**(3): p. 402-4.

53.   Ma, W., et al., *Usefulness of external counterpulsation early postoperatively after the Fontan procedure in children.* Am J Cardiol, 2002. **90**(9): p. 1029-31.

54.   Loh, P.H., et al., *Enhanced external counterpulsation in the treatment of chronic refractory angina: a long-term follow-up outcome from the International Enhanced External Counterpulsation Patient Registry.* Clin Cardiol, 2008. **31**(4): p. 159-64.

55.   Butson, A.R., *The clinical use of antishock trousers.* Can Med Assoc J, 1983. **128**(12): p. 1428-30.

56.   Werner, D., et al., *Impact of enhanced external counterpulsation on peripheral circulation.* Angiology, 2007. **58**(2): p. 185-90.

57.   Kemeny, A. and L.A. Geddes, *Retrospectroscope. Military antishock trousers.* IEEE Eng Med Biol Mag, 2005. **24**(4): p. 80, 91.

58.   Committee, O.M.C., *2008 Prehospital Patient Care Protocols*, O.D.E. Alliance, Editor. 2008.

59.   Riaz, A. *EECP Heart Clinic*. 2008 [cited 2010.

60. Miyazoe, Y., T. Sawairi, K. Ito, et al., *Computational Fluid Dynamic Analyses to establish design process of centrifugal blood pumps.* Artif Organs, 1998(23): p. 381-385.

61. Bhavsar, S.S., et al., *Intravascular mechanical cavopulmonary assistance for patients with failing Fontan physiology.* Artif Organs, 2009. **33**(11): p. 977-87.

62. Throckmorton, A.L., et al., *Numerical design and experimental hydraulic testing of an axial flow ventricular assist device for infants and children.* ASAIO J, 2007. **53**(6): p. 754-61.

63. Takiura, K., T. Masuzawa, S. Endo, et al., *Development of design methods of a centrifugal blood pump with in virto test, flow visualization, and computational fluid dynamics:results in hemolysis tests.* Artif Organs, 1998(22): p. 393-398.

64. Wendt, J., *Computational Fluid Dynamics: An Introduction.* 1992, Berlin, Germany: Springer-Verlag.

65. Ryu, K., T.M. Healy, A.E. Ensley, S. Sharma, C. Lucas, A.P. Yoganathan, *Importance of Accurate Geometry in the study of the Total Cavopulmonary Connection: Computational Simulations and in vitro Expirements.* . Annals of Biomedical Engineering, 2001(29): p. 844-853.

66. Throckmorton, A.L. and A. Untaroiu, *CFD analysis of a Mag-Lev ventricular assist device for infants and children: fourth generation design.* ASAIO J, 2008. **54**(4): p. 423-31.

67. Elder, R., A. Tourlidakis, M Yates, *Advances of CFD in Fluid Machinery Design.* 2003, Hoboken, NJ: John Wiley and Sons, Inc.

68. Warsi, Z., *Fluid Dynamics: Theoretical and Computational Approaches.* 1999, Boca Raton, FL: CRC Press.

69. Kundu, P.J., I.M. Cohen, *Fluid Mechanics.* 4th Edition. 2008, Burlington, MA: Elsevier Inc.

70. Long, J.A., et al., *Viscoelasticity of pediatric blood and its implications for the testing of a pulsatile pediatric blood pump.* ASAIO J, 2005. **51**(5): p. 563-6.

71. Throckmorton A.L., R.K., *Design of a protective cage of filaments for an axial flow blood pump for intravascular cavopulmonary assist.* Artif Organs, 2009(33): p. 611-621.

72.   Merrill, E.W. and G.A. Pelletier, *Viscosity of human blood: transition from Newtonian to non-Newtonian.* J Appl Physiol, 1967. **23**(2): p. 178-82.

73.   Cokelet, G.R., *Rheology and hemodynamics.* Annu Rev Physiol, 1980. **42**: p. 311-24.

74.   Cokelet, G.R., *Experimental determination of the average hematocrit of blood flowing in a vessel.* Microvasc Res, 1974. **7**(3): p. 382-4.

75.   Paul, R., et al., *Shear stress related blood damage in laminar couette flow.* Artif Organs, 2003. **27**(6): p. 517-29.

76.   Song, X., A.L. Throckmorton, H.G. Wood, J.F. Antaki, D.B. Olsen, *Quantitative evaluation of blood damage in a centrifugal VAD by computational fluid dynamics.* J Fluids Eng, 2004(126): p. 410-418.

77.   Bludszuweit, C., *Three-dimensional numerical prediction of stress loading of blood particles in a centrifugal pump.* Artif Organs, 1995. **19**(7): p. 590-6.

78.   Heuser, G., R. Opitz, *A couette viscometer for short time shearing in blood.* Biorheology, 1980(17): p. 17-24.

79.   Song, X., A.L. Throckmorton, H.G. Wood, J.F. Antaki, D.B. Olsen, *Computational Fluid Dynamics Prediction of Blood Damage in a Centrifugal Pump.* Artif Organs, 2003. **27**(10): p. 938-941.

80.   Koller, T., Jr. and A. Hawrylenko, *Contribution to the in vitro testing of pumps for extracorporeal circulation.* J Thorac Cardiovasc Surg, 1967. **54**(1): p. 22-9.

81.   Kawahito, S., et al., *Blood trauma induced by clinically accepted oxygenators.* ASAIO J, 2001. **47**(5): p. 492-5.

82.   Naito, K., K. Mizuguchi, and Y. Nose, *The need for standardizing the index of hemolysis.* Artif Organs, 1994. **18**(1): p. 7-10.

83.   Mitamura, Y., H. Nakamura, K. Sekine, et al., *Prediction of hemolysis in rotary blood pumps with computational fluid dynamics analysis.* Journal of Congestive Heart Failure and Circulatory Support, 2001(4): p. 331-336.

84.   Ng, A.V., P. Hanson, E.A. Aaron, R.B. Bemment, J.M. Conviser, F.J. Nagle, *Cardiovascular response to military antishock trouser inflation during standing arm exercise. .* Journal of Applied Physiology, 1987. **63**(3): p. 1124-1129.

85.   Michaels, A.D., et al., *Left ventricular systolic unloading and augmentation of intracoronary pressure and Doppler flow during enhanced external counterpulsation.* Circulation, 2002. **106**(10): p. 1237-42.

86.   Fontan, F., C. Deville, J. Quaegebeur, et al., *Repair of tricuspid atresia in 100 patients.* journal of Thoracic Cardiovascular Surgery, 1983. **85**: p. 647-660.

87.   Fontan, F.E.B., *Surgical Repair of Tricuspid Atresia.* Thorax, 1971. **26**: p. 240-248.

88.   Yoshiki, M., M. Shoji, T. Nakanishi, T. Fujii, M. Nakazawa, *Elevated vascular endothelial growth factor levels are associated with aortopulmonary collateral vessels in patients before and after the Fontan procedure.* American Heart Journal, 2007. **153**: p. 987-994.

89.   DeBakey, M.E., *A miniature implantable axial flow ventricular assist device.* Ann Thorac Surg, 1999. **68**(2): p. 637-40.

90.   Catena, E., et al., *Three-dimensional echocardiographic assessment of a patient supported by intravascular blood pump Impella recover 100.* Echocardiography, 2005. **22**(8): p. 682-5.

91.   Lee, M.S. and R.R. Makkar, *Percutaneous left ventricular support devices.* Cardiol Clin, 2006. **24**(2): p. 265-75, vii.

92.   Arieti, M., G. Pesarini, and F. Ribichini, *Percutaneous Impella Recover circulatory support in high-risk coronary angioplasty.* Cardiovasc Revasc Med, 2008. **9**(4): p. 269-74.

93.   Whitehead, K.K., K. Pekkan, H.D. Kitajima, S.M. Paridon, A.P. Yoganathan, M.A. Fogel, *Nonlinear power loss during exercise in single-ventricle patient after the Fontan: insights from computational fluid dynamics.* Circulation, 2007. **116**(Suppl. I): p. I165-I171.

APPENDIX A: MAST STUDY PROTOCOL

MAST Study Protocol:

1. After obtaining consent, place patient supine in MAST garment. MAST are not inflated.
2. Place blood pressure cuff, pulse oximeter, standard ECG leads on patient. Insert catheter according to VCU protocol for cardiac catherization.
3. Obtain and record baseline measurements onto data sheet. Based upon the patient's diastolic pressure, determine three pressure levels to evaluate:

   1st Pressure level = (Diastolic BP) – 10 mmHg

   2nd Pressure level = (Diastolic BP)

   3rd Pressure level = (Diastolic BP) + 10 mmHg
4. Administer the first pressure level with the following procedure:
   * Note: Clinical Measurements should be ongoing during this time.
   1. Use pump to inflate MAST garment to 1st pressure level.
   2. Hold pressure for 10 – 15 seconds.
   3. Release pressure valve and deflate pants.
   4. Hold deflated for 10 – 15 seconds.
   5. Repeat cycle 5 times.
   6. During the 5th cycle, reassess patient's vital signs prior to deflation.
   7. Conclude after 5 minutes of Counterpulsation cycles.
   8. Allow patient to rest for 3-5 minutes.
5. Administer the second pressure level with the following procedure:
   * Note: Clinical Measurements should be ongoing during this time.
   1. Use pump to inflate MAST garment to 1st pressure level.
   2. Hold pressure for 10 – 15 seconds.
   3. Release pressure valve and deflate pants.
   4. Hold deflated for 10 – 15 seconds.
   5. Repeat cycle 5 times.
   6. During the 5th cycle, reassess patient's vital signs prior to deflation.
   7. Conclude after 5 minutes of Counterpulsation cycles.
   8. Allow patient to rest for 3-5 minutes.
6. Administer the third pressure level with the following procedure:
   * Note: Clinical Measurements should be ongoing during this time.
   1. Use pump to inflate MAST garment to 1st pressure level.

2. Hold pressure for 10 – 15 seconds.
3. Release pressure valve and deflate pants.
4. Hold deflated for 10 – 15 seconds.
5. Repeat cycle 5 times.
6. During the 5th cycle, reassess patient's vital signs prior to deflation.
7. Conclude after 5 minutes of Counterpulsation cycles.
8. Allow patient to rest for 3-5 minutes.
7. After the patient rests for 5 minutes, reevaluate baseline vital signs.

APPENDIX B: RESEARCH SUBJECT CONSENT FORM

RESEARCH SUBJECT INFORMATION AND CONSENT FORM

TITLE OF RESEARCH: Clinical Measurement of Pressure Augmentation in the Systemic Venous Circulation using Medical Anti-Shock Trousers

VCU IRB PROTOCOL NUMBER:

INVESTIGATORS:
<u>Principal Investigator</u>: Amy Throckmorton, Ph.D.
Sub/Co-Investigator: William B. Moskowitz, M.D.
Sub/Co-Investigator: Scott D. Gullquist, M.D.
Student: Sonya Bhavsar, B.S.

In ordinance with Federal Regulations for the Protection of Human Subjects section §46.116, "An investigator shall seek…consent only under circumstances that provide the prospective subject or the representative sufficient opportunity to consider whether or not to participate and that minimize the possibility of coercion or undue influence." **After carefully reading and understanding the information listed below, if you would like to participate in this research study please sign this consent form indicating your consent.**

This consent form may contain words or information that you do not understand. Please ask one of the investigators to explain any words or information that you do not understand. You may take home an unsigned copy of this consent form to think about or discuss with family or friends before making your decision.

PURPOSE OF THE RESEARCH STUDY:
The purpose of this research study is the test the effectiveness of routinely administered, non-invasive, external couterpulsation therapy via Medical Anti-Shock Trousers (MAS

trousers). MAS trousers are pants that have an air filled gap inside of them; they function similar to blood pressure cuffs and can be inflated, only around the lower extremities or legs, as opposed to the upper arm. We will have you slip on the pants and then, using air, inflate these trousers. This will apply an external pressure to your legs in the form of light compression. In doing so, we will measure how this externally applied pressure may modify blood flow conditions in the circulation on the right side of your heart.

You are being invited participate in this study because you have been diagnosed with single ventricle physiology or a closely related congenital heart defect and have already scheduled to receive an evaluative cardiac catheterization. Therefore, we can perform this study right before your cardiac catheterization in a safe and efficient manner.

WHAT YOU WILL DO IN THE STUDY:
Your participation in this study will last approximately 20 minutes per session. We will acquire baseline vitals (blood pressure, heart rate, O_2 saturation, respirations, right atrial pressure/central venous pressure, and pulmonary capillary wedge pressure) prior to inflating the pants with air, followed by three 3-5 minute sessions of incrementally increasing inflation levels. Your vital signs will be monitored throughout the session and again approximately 5 minutes after completion to obtain a second set of baseline vitals.

Sample Procedural Timeline:

1.) You will be placed in laying down, flat on your back. The MAS trousers will be applied.
2.) We will apply a blood pressure cuff, pulse oximeter, and ECG leads. A catheter will be inserted into your femoral vein after the site has been numbed with local anesthetic.
3.) Your first set of vital signs will be obtained. We will determine the three pressure intervals based upon your diastolic blood pressure.
4.) The first pressure level will be administered. The MAS trousers will inflate and you will feel circumferential pressure applied to your lower extremities similar to a blood pressure cuff.
5.) Your vital signs will be reassessed and the MAS trousers will deflate. You will rest for 3-5 minutes.
6.) The second pressure level will be applied which is slightly higher than the previous.
7.) Your vital signs will again be reassessed and the MAS trousers will deflate. You will rest for 3-5 minutes.
8.) The third and final pressure level will be applied, your vital signs will be assessed and the MAS trousers will deflate.
9.) After 5 minutes a second set of baseline vitals will be obtained.

Your participation in this study will last approximately 20 minutes. Approximately 10 subjects will participate in this study.

RISKS AND RISK REDUCTION:
Prior to your enrollment in the study, an exclusion criteria was established to minimize any potential risks. Because you have been invited to participate in this study, you were determined to be at little to no risk.

Due to the short time period of external pressure application, there is minimal to no risk. Deflation of the MAS trousers will be done methodically in order to maintain cardiac stabilization. Your vital signs will be carefully monitored and adjustments will be made as necessary.

You will also be carefully monitored for any sign or symptoms of shock, which will be highly unlikely given the short duration (1-2 minutes) of externally applied pressure. Significant concern would arise if the duration of applied pressure exceeded 20 minutes, and the pressure was rapidly released, which will not occur during this study. Investigators and a full clinical staff in the cardiac catheterization lab will be present to ensure that the protocol will not be violated.

During the procedure, we will determine whether positive results are being observed. If the observed results are not compliant with the hypothesized results, the procedure and study will be immediately terminated.

All key personnel and resources normally found in the cardiac catheterization lab will be present and attentive during the course of procedure.

BENEFITS TO YOU AND OTHERS:
There is no guarantee that you will receive any medical benefits from being in this study.

This is not a treatment study, and you may not receive any direct medical benefits from your participation. The information from this research study may lead to better treatment in the future for patients with single ventricle physiology or a closely related congenital heart defect.

COMPENSATION:
No compensation will be provided for this study. The knowledge gained from this study will be used to develop new MAS trousers or counterpulsation technology as a clinical management tool for patients with single ventricle physiology or a closely related congenital heart defect similar to yours.

CONFIDENTIALITY
Adhering to IRB and Federal HIPPA regulations, only nonspecific information will be recorded during this study. This information includes patient age, sex, and diagnosis.

Data being collected is for research purposes only. Your data will be identified by ID numbers, **NOT** names, and stored separately from medical records in a secured spreadsheet with the principle investigator.

Access to all data will be limited to study personnel. A data and safety monitoring plan is established with accordance to IRB and Federal HIPPA regulations.

COMPENSATION FOR INJURY:
Virginia Commonwealth University and the VCU Health System have no plan for providing long-term care or compensation in the event that you suffer injury as a result of your participation in this research study.

If you are injured or if you become ill as a result of your participation in this study, contact one of your investigators immediately. Your investigator will arrange for short-term emergency care or referral if it is needed.

Fees for such treatment may be billed to you or to appropriate third party insurance. Your health insurance company may or may not pay for treatment of injuries as a result of your participation in this study.

VOLUNTARY PARTICIPATION AND WITHDRAWAL:
Your participation in this study is voluntary. If you decide to not participate in this study, you will not suffer any penalty or loss of benefits to which you are otherwise entitled. If you do participate, you are free to withdraw at any time. Your decision to withdraw will involve no penalty or loss of benefits to which you are otherwise entitled.

Your principle investigator, co-investigators, or student investigator can stop your involvement in the study at anytime without your consent. This could occur due to:
  1.) The investigators believe it to be necessary for your health or safety
  2.) You failed to comply with study instructions
  3.) Administrative reasons requiring your withdrawal

QUESTIONS:
If you have any questions about this study, contact:

Amy L. Throckmorton, Ph.D.

Assistant Professor

Department of Mechanical Engineering

Virginia Commonwealth University

VCU Box # 843015

Office (804)-827-2278

Fax (804)-827-7030

althrock@vcu.edu

William B. Moskowitz, M.D.

Professor, Pediatrics and Medicine

Interim Chair, Department of Pediatrics

Chairman, Division of Pediatric Cardiology

VCU/Medical College of Virginia

VCU Box #980646

Office (804)-828-9143

wmoskowitz@mcvh-vcu.edu

Scott D. Gullquist, M.D.

Associate Professor, Pediatric Cardiology

Department of Pediatrics

VCU/Medical College of Virginia

VCU Box #980646

Office (804)-828-5745

sgullquist@mcvh-vcu.edu

Sonya Bhavsar, B.S.

Graduate Student Research Assistant

Department of Mechanical Engineering

Virginia Commonwealth University

Mobile (540)-915-1248

bhavsarss@vcu.edu

If you have questions about your rights as a research subject, you may contact:

Office of Research
Virginia Commonwealth University
800 East Leigh Street, Suite 113
PO Box 980568
Richmond, VA 23298
(804) 827-2157

Do not sign this assent/consent form unless you have had a chance to ask questions and have received satisfactory answers to all of your questions. Additional information about participation in research studies can be found at:
http://www.research.vcu.edu/irb/volunteers.htm

ASSENT for a patient between the ages of 7 and 12

I agree to be in a study that uses MAS trousers (pants that inflate with air like a blood pressure cuff) to determine changes in blood flow to the heart. This study was explained to me by my parent/guardian and the doctor. They said that I could be in it. The only people who will know about my results will be the people in charge of the study.

In this study I will put on a pair of pants that inflate with air like blood pressure cuffs. I will be lying on my back. The doctor, nurses, and people in charge will be watching me closely to make sure I am ok during the study. The pants will inflate and squeeze lightly on both of my legs three times. It will only take about 20 minutes. If I ever feel uncomfortable, I will tell the doctor and he will stop the study.

Writing my name below means that this page was read by me or to me and that I agree to be in this study. I know what will happen to me during the study. If I decide to quit the study, all I have to do is tell the person in charge.

_____   _____

Child's Signature   Date

_____

Name of Person Conducting Informed Assent

_____   _____

Signature of Person Conducting Informed Assent   Date

_____   _____

Signature of Investigator (if different from above)   Date

ASSENT for a patient between the ages of 13 and 17

"I have read the description of the study titled Clinical Measurement of Pressure Augmentation in the Systemic Venous Circulation using Medical Anti-Shock Trousers which is printed above. I understand the procedures and what will happen to me in the study. I have received permission from my parent(s) to participate in the study, and I agree to participate in it. I know that I can quit the study at any time."

_____   _____

Signature of Child   Date

CONSENT

I have been provided with an opportunity to read this consent form carefully. All of the questions that I wish to raise concerning this study have been answered.

By signing this consent form, I have not waived any of the legal rights or benefits, to which I otherwise would be entitled. My signature indicates that I freely consent to participate in this research study. I will receive a copy of the consent form once I have agreed to participate.

Please read if you are the Parent/Legal Guardian of a patient participating in this study:
You are making the decision to allow your child to participate in this study. Your signature below indicates that you have read the information provided above and have decided to allow him or her to participate in this study. If your child is between the ages of 7 and 12, your signature below indicates that you have talked with your child about the study and believe he or she fully understands what will happen during the study. If you later decide that you wish to withdraw your permission for your child to participate in the study, simply tell an investigator or the doctor. You may discontinue his or her participation at any time.

_____
Subject Name, printed

_____ _____
Subject Signature   Date

_____
Name of Parent or Legal Guardian
(Printed)

_____ _____
Parent or Legal Guardian Signature   Date

_____
Name of Person Conducting Informed Assent/Consent
Discussion / Witness
(Printed)

_____ _____
Signature of Person Conducting Informed Assent/Consent   Date
Discussion / Witness

_____ _____
Investigator Signature (if different from above)   Date

VITA

Sonya Sanat Bhavsar was born on January 13, 1986 in Trenton, New Jersey and is a citizen of the United States of America. She graduated from Hidden Valley High School in Roanoke, Virginia in 2004 and received her Bachelor of Science in Biomedical Engineering from Virginia Commonwealth University in Richmond, Virginia in 2008. During her undergraduate education Sonya worked as a research assistant at the Massey Cancer Center in the Molecular Cancer Therapeutics Programs in 2006 and the VCU/MCV Nursing School PRO Study in 2007.

In the fall of 2008, Sonya entered her Masters program in Mechanical Engineering at Virginia Commonwealth University. She worked as a research assistant in the BioCirc Laboratory under the direction of Dr. Amy Throckmorton. Sonya also worked as a teaching assistant and part time as an Orthopedic Care Partner at the Medical College of Virginia. She served as the president of the Society of Women Engineers and founding member and president of American Society of Artificial Internal Organs:fyi student chapter. Sonya also volunteered her time to the community as an Emergency Medical Technician at Lakeside Volunteer Rescue Squad where she is the chief financial officer, board member, and squad leader.

During her graduate work, Sonya was honored as the recipient of the 2009 Biomedical Engineering Graduate Student award at the 5th International Conference of Pediatric Mechanical Circulatory Support Systems and Pediatric Cardiopulmonary Perfusion Conference. She was also honored as a 2010 VCU I-GEEAR GAAN fellow and recipient of the 2010 Susan E. Kennedy Scholarship. Sonya was co-author on several publications, professional conference presentations, and professional poster presentations including being first author on "Intravascular Mechanical Cavopulmonary Assistance for Patient with Failing Fontan Physiology", "Interaction of an Idealized Cavopulmonary Circulation with Mechanical Circulatory Assist using an Intravascular Rotary Blood Pump", "Use of External Pressure Application to Augment Fontan Hemodynamics", and several others.